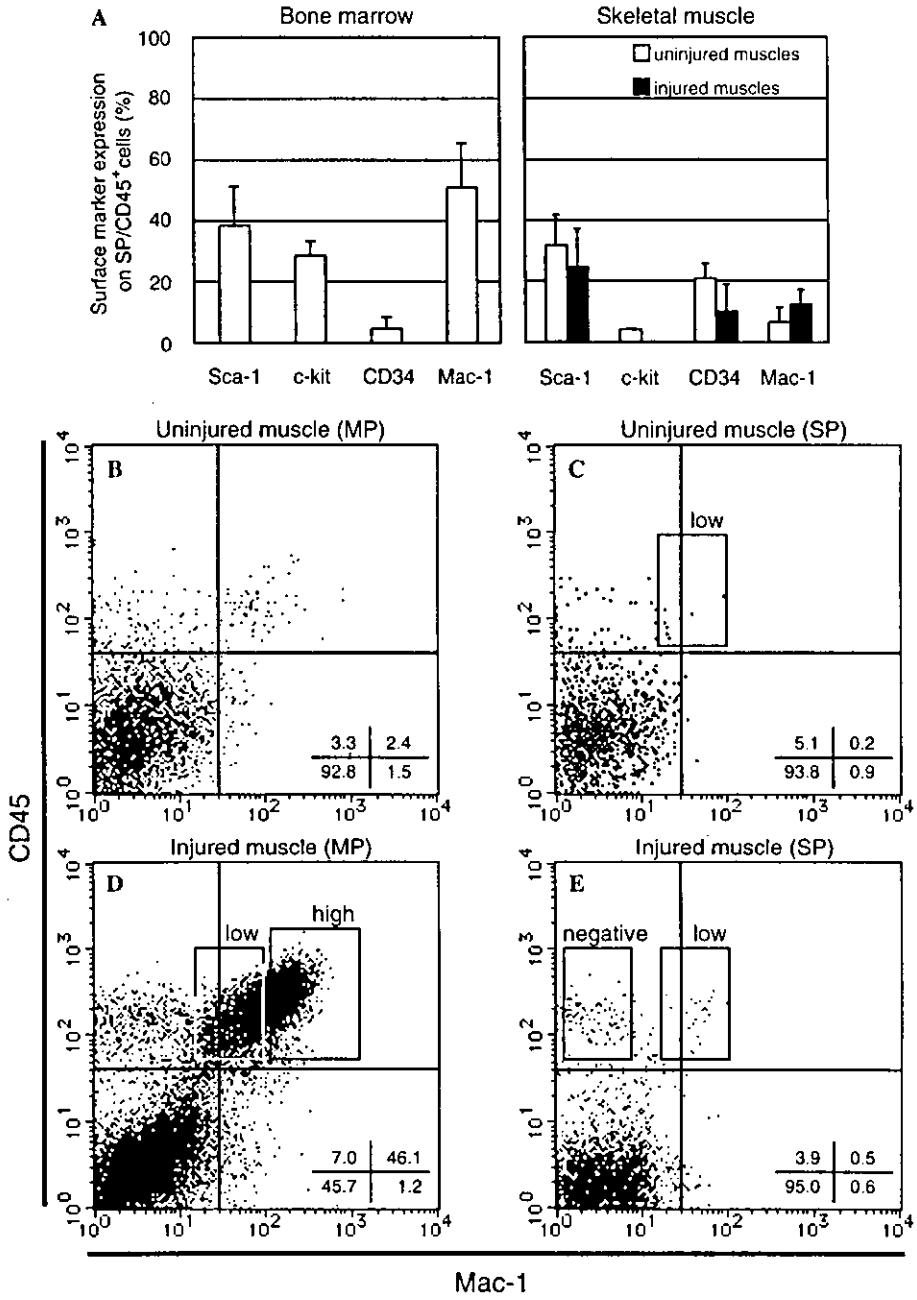

Fig. 3. Analysis of surface marker expression on BM-derived SP/CD45$^+$ cells prepared from muscles. (A) SP cells from BM (left graph), BM-derived SP cells from uninjured (white columns in right graph), and BM-derived SP cells from injured muscles (black columns in right graph) were isolated and then stained with anti-CD45 antibody and one of the following markers: Sca-1, c-kit, CD34, or Mac-1. The percentages of surface marker expression on BM-SP/CD45$^+$ cells (left graph) and on BM-derived SP/CD45$^+$ cells (right graph) were calculated by the following formula: (%) = 100 × (the number of surface marker-positive CD45$^+$ cells in the SP fraction)/(the number of CD45$^+$ cells in the SP fraction). Note that the expression of c-kit in BM-derived SP/CD45$^+$ cells from injured muscles was not at a detectable level. All values (means ± SD) are based on at least three separate experiments. (B–E) Representative FACS analysis demonstrating that mononucleated cells in the MP fraction (B,D) or the SP fraction (C,E) isolated from uninjured muscles (B,C) or injured muscles (D,E) of the *GFP* transgenic mice. In injured muscles, MP/CD45$^+$ cells expressed Mac-1 with a broad range of intensities (D). By contrast, the SP fraction from injured muscles contained not CD45$^+$ Mac-1^{high} cells but CD45$^+$ Mac-1^{low} cells (E). Importantly this SP/D45$^+$ Mac-1^{low} fraction increased in cell number as well as in ratio after muscle injury (rectangles marked "low" in C,E; also see A). The SP sub-fractions shown by rectangles in (D,E) were isolated and then used in further culture experiments (see Fig. 4 and Table 3).

and anti-sarcomeric α-actinin antibody (Figs. 4D–F). BM-derived SP cells gave rise to myotubes more effectively than BM-derived MP cells (Table 3). In particular, the BM-derived SP/CD45$^+$ Mac-1^{low} fraction was highly concentrated in cells capable of myotube formation (Table 3). More importantly, sarcomeric α-actinin-expressing mononucleate myocytes were observed in our co-culture system (Figs. 4G–J), indicating that

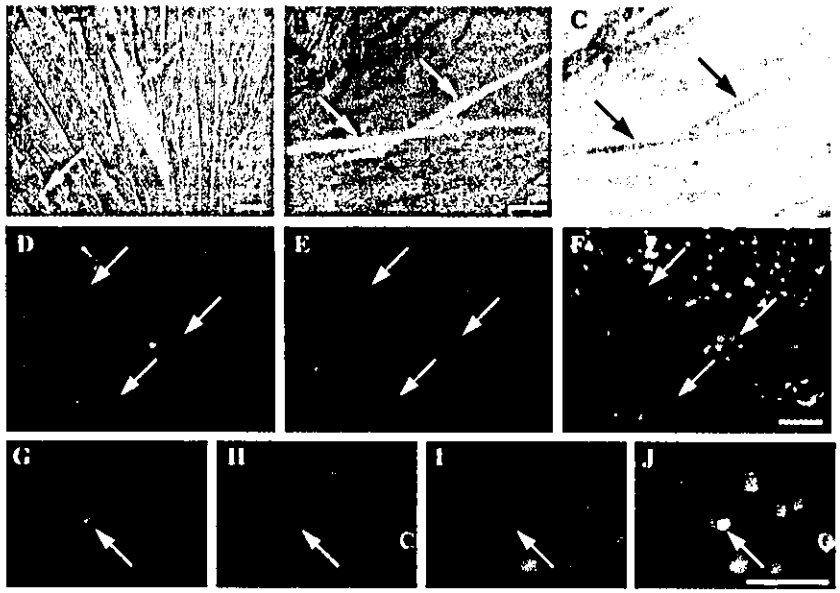

Fig. 4. Myogenic differentiation of BM-SP/CD45$^+$ cells and BM-derived SP/CD45$^+$ Mac-1^{low} cells from regenerating muscles. (A) GFP$^+$ BM-SP/CD45$^+$ cells isolated from *GFP* transgenic mice were co-cultured with activated satellite cells from C57BL/6 mice. GFP$^+$ multinucleated myotubes (arrows) were observed after 14 days of co-culture. (B,C) GFP$^+$ BM-SP/CD45$^+$ cells were co-cultured with activated satellite cells prepared from ROSA26 mice. (B) A representative image of living GFP$^+$ myotubes at 21 days co-culture. (C) After fixation, cells were counterstained with X-gal. Arrows show heterokaryotic myotubes expressing both GFP and β-galactosidase. (D–J) Co-culture of GFP$^+$ BM-derived SP/CD45$^+$ cells from injured muscles of *GFP* transgenic mice with activated satellite cells from C57BL/6. Immunofluorescent staining for GFP (D,G and green in F,J), sarcomeric α-actinin (E,H and red in F,J), and Hoechst 33258 (I, blue in F,J) at 14 days co-culture of BM-derived SP/CD45$^+$ Mac-1^{low} cells (a rectangle indicates "low" in Fig. 3E) from regenerating muscles of the *GFP* transgenic mice with activated satellite cells of C57BL/6 mice. (D–F) Arrows indicate GFP$^+$ multinucleate myotubes expressing sarcomeric α-actinin. (G–J) Arrows indicate a GFP$^+$ mononucleated cell expressing sarcomeric α-actinin. Note that a mononucleated cell derived from the GFP$^+$ SP/CD45$^+$ Mac-1^{low} fraction differentiated into a myogenic cell before fusion with host muscle cells (arrows). Bars, 50 μm.

Table 3
Frequency of GFP$^+$ myotube formation in co-culture with activated satellite cells

Cultured cells		No. of experiments	No. of cells seeded	No. of GFP$^+$myotubes	Frequency of GFP$^+$myotubes (%)[a]
Tissue	Cell type				
Regenerating muscle	SP/CD45$^+$	2	21,500	51	0.24
	SP/CD45$^+$Mac-1$^-$	3	23,000	65	0.28
	SP/CD45$^+$Mac-1^{low}	3	6600	34	0.52
	MP/CD45$^+$	2	20,000	4	0.02
	MP/CD45$^+$Mac-1^{low}	3	62,700	44	0.07
	MP/CD45$^+$Mac-1^{high}	3	70,500	19	0.03

[a] % = (the number of GFP$^+$ myotubes/the number of seeded cells) × 100.

BM-derived SP/CD45$^+$ Mac-1^{low} cells from regenerating muscles had the ability to differentiate into skeletal muscle cells and did not simply fuse with host myogenic cells to form heterokaryotic myotubes. Although BM-derived MP/CD45$^+$ Mac-1^{high} cells formed myotubes at low frequency, we have not observed mononucleate myocytes from MP/CD45$^+$ Mac-1^{high} cells in our co-culture system. We next injected BM-derived SP/CD45$^+$ Mac-1^{low} cells from regenerating muscles into TA muscles of NOD-scid mice, and we detected a few GFP-positive fibers (not shown).

Discussion

Contribution of BM cells to muscle fiber regeneration

The number of donor-derived muscle fibers normalized to the number of transplanted cells was significantly higher in BM-SP/CD45$^+$ cell-transplanted mice than in unfractionated BM cell-transplanted mice. These results suggest that cells with myogenic potential are enriched in the BM-SP/CD45$^+$ cell fraction. We and other groups [6,8,12,13,15,18,22] have observed that muscle damage

increased the frequency of donor-derived myofibers in mice. Thus, muscle damage and subsequent regeneration could be important for the participation of donor-derived cells in skeletal muscle regeneration and, in particular, for recruitment of BM cells to damaged muscle.

Migration of SP cells from BM to regenerating muscles

We showed, for the first time, that a considerable number of SP cells migrated from BM to regenerating muscle together with inflammatory cells such as monocytes/macrophages at the early stage of muscle regeneration. The release of a variety of cytokines/chemokines into regenerating muscle [19] suggests that certain kinds of chemotactic factors, which have an analogous mechanism to monocytes/macrophages, recruit BM-SP cells to regenerating muscles. At this stage of muscle regeneration, satellite cells are activated and proliferate enormously to form fully matured multinucleated cells [3]. Hence, regenerating muscles could provide opportunities for BM-derived SP cells to come into contact with myogenic cells.

Absence of hematopoietic stem and/or progenitor cells in the BM-derived SP fraction isolated from regenerating muscles

One of the most interesting aspects of BM-derived SP cells in regenerating muscles is the lack of hematopoietic potential. It has been reported that BM-SP cells were able to reconstitute the hematopoietic system in lethally irradiated mice [16,17]. In fact, in our transplantation, 2000 BM-SP/CD45$^+$ cells reconstituted the hematopoietic system in mice. Likewise, at least 137 uninjured muscle-derived SP/CD45$^+$ cells have been reported to reconstitute the mouse blood system [23]. However, 3000 SP/CD45$^+$ cells isolated from regenerating muscles in this study failed to reconstitute the blood system in recipients. Uninjured muscles contained c-kit$^+$ BM-derived SP cells (our results [23]), even if the level of c-kit expression detectable was low. BM-derived SP cells from injured muscles did not expressed c-kit antigen, although c-kit is one of the key surface markers for hematopoietic stem and/or hematopoietic progenitor cells [26]. Therefore, our results suggest that BM-derived SP cells in regenerating muscles contain neither HSCs nor hematopoietic progenitors.

Early myeloid cells in the BM-derived SP fraction of regenerating muscles

Scharenberg et al. [32] have reported that BM-SP cells sharply down-regulated *ABCG2* at the stage of lineage commitment, resulting in loss of the SP phenotype. In fact, our surface marker analysis revealed that BM-derived SP cells from regenerating muscles did not contain either Mac-1^{high} or F4/80$^+$ cells, which are mature inflammatory cells, but did contain Mac-1^{low} cells. In addition, it has been reported that early myeloid cells expressed a low level of Mac-1 antigen [1,29,30]. Therefore, the BM-derived SP fraction should contain early myeloid cells rather than mature inflammatory cells. Our results showed that these early myeloid (BM-derived SP/CD45$^+$ Mac-1^{low}) cells were considerably mobilized to muscles after injury.

Enrichment of cells with myogenic differentiation in BM-derived SP/CD45$^+$ Mac-1^{low} cells

Camargo et al. [6] demonstrated that myeloid intermediates were incorporated into myofiber formation in response to injury using the lysozyme-M/Cre transgene tracing strategy. More recently, it was shown that the expression of lysozyme-M does not specifically mark cells with myeloid commitment but marks all kinds of hematopoietic cells in their transgene tracing strategy [36]. Hence, it remained unclear what types of cell fractions in BM-derived cells were incorporated into myotubes/myofibers. Here, our co-culture studies clearly revealed that isolated BM-derived SP/CD45$^+$ Mac-1^{low} fraction prepared from regenerating muscles showed the highest myogenic differentiation ability among several BM-derived fractions. In addition, BM-derived cells abruptly lost their myogenic differentiation efficiency after they lost the SP phenotype, suggesting that the myotube formation efficiency of BM-derived cells from regenerating muscles was dependent on their maturation stage.

Zhao et al. [39] have shown that monocytes in peripheral blood differentiated into various cell types under their specific differentiation conditions. In addition, BM-derived myogenic progenitors transiently expressed the low level of Mac-1 antigen at the early process of muscle differentiation [25]. Their results together with ours suggest that BM-derived early myeloid cells might convert to other cell lineages including the myogenic cell lineage in certain circumstances, such as regenerating muscles. Our direct transplantation of muscle-derived Mac-1^{low} SP cells from GFP transgenic mice into TA muscles of NOD-scid mice, however, resulted in low efficient GFP-positive myotube formation (data not shown). Although a considerable number of injected cells die shortly after the injection due to innate immune response by the host, the results, together with in vitro co-culture experiments (GFP-positive myotube formation rate: ave. 0.52%), indicate that the efficiency of myogenic conversion of Mac-1^{low} SP cells is relatively low, compared with muscle satellite cells.

Myogenic differentiation mechanism of SP cells

Our co-culture studies revealed that BM-derived SP cells as well as BM-SP cells formed myotubes with host

myogenic cells. Importantly, we found skeletal muscle-specific protein expressing mononucleate myocytes that originated from BM-derived SP/CD45^{+} Mac-1^{low} cells in regenerating muscles. This result strongly suggests that BM-derived SP cells commit to the myogenic cell lineage before fusion with host myogenic cells and that this myogenic contribution is not a random but a stepwise progressive event. A subset of SP cells would adjust to a new environment and start a myogenic differentiation program. Probably its trigger is cell-to-cell contact between SP cells and myogenic cells rather than soluble factors, because conditioned medium of cultured myogenic cells had no effect on myogenic differentiation of SP cells in vitro (data not shown). In addition, we have not observed myotubes in cultures of SP cells alone (data not shown).

Taken together, our results revealed that early myeloid cells in the BM-derived SP fraction are implicated in skeletal muscle regeneration in the presence of pre-existing myogenic cells. In our proposed model (Fig. 5), a large number of BM-derived SP cells migrate to regenerating muscles in response to injury. These mobilized

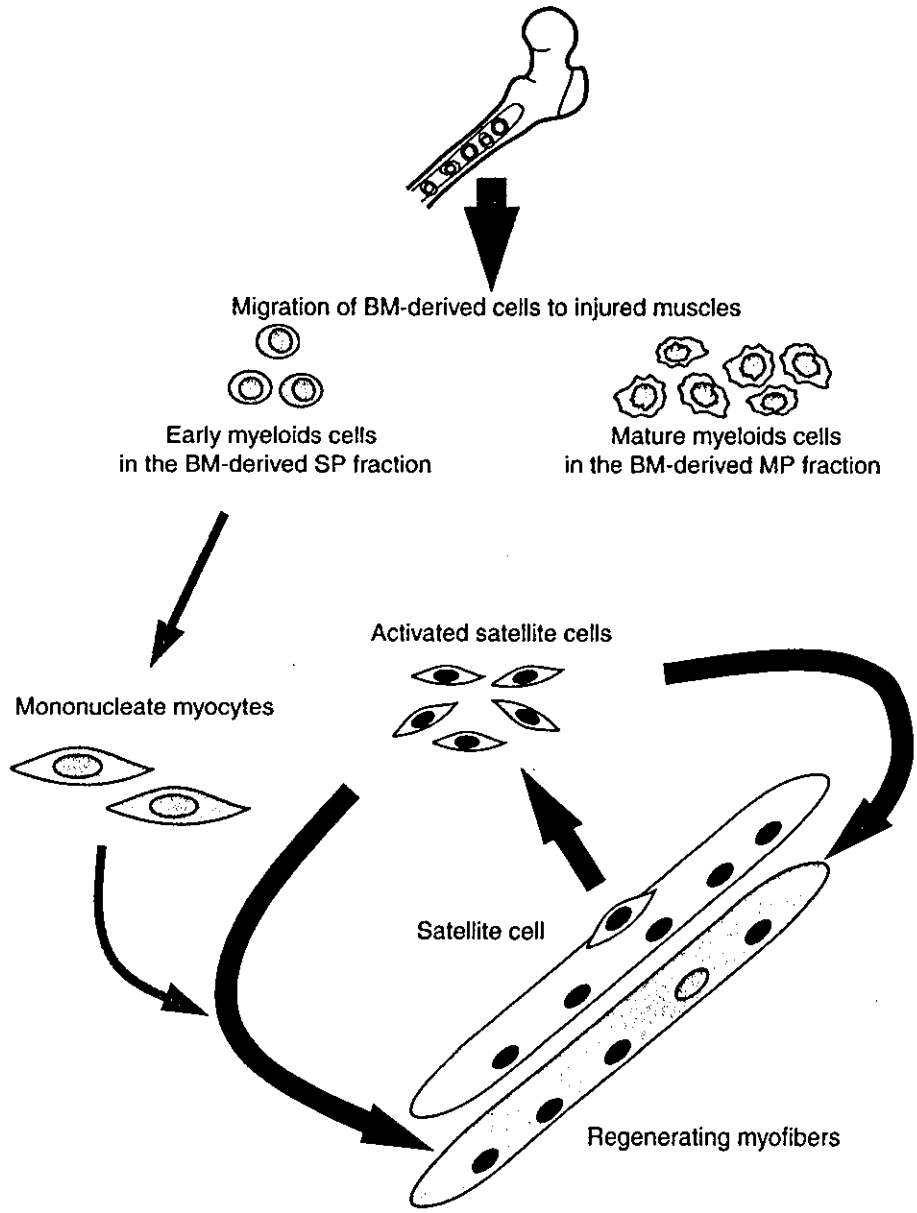

Fig. 5. Model for BM-derived SP cell-mediated muscle regeneration. In response to injury, BM-derived cells are mobilized to injured muscles (gray arrows). Neither HSCs nor hematopoietic progenitors migrate to injured muscles. Migrated BM-derived SP cells in regenerating muscles contain early myeloid cells that enrich cells with myogenic differentiation. These early myeloid cells advance toward mature multinucleated myotubes/myofibers via a myogenic differentiation program before fusion with myogenic cells (blue arrows). On the other hand, some mature macrophages might be stochastically incorporated into myotubes/myofibers at low efficiency.

BM-derived SP cells contain early myeloid cells that enrich cells capable of myogenic differentiation. In regenerating muscles, they advance toward mononucleated myocytes before fusion with pre-existing myogenic cells. They probably require cell-to-cell contact with myogenic cells for skeletal muscle differentiation. The molecular mechanism by which skeletal muscle cells are induced to fuse with BM-derived SP cells and to differentiate BM-derived SP cells into myogenic cells remains to be determined.

Acknowledgments

We are grateful to colleagues in our laboratory, in particular Dr. S. Fukada, for useful discussion and suggestions on this work. K.O. is supported by a Research Fellowship from the Japan Society for the Promotion of Science. This work is supported by Grants-in-Aid for Center of Excellence (COE), Research on Nervous and Mental Disorders (10B-1, 13B-1), and Health Sciences Research Grants for Research on the Human Genome and Gene Therapy (H10-genome-015, H13-genome-001) from the Ministry of Health, Labor and Welfare of Japan, and a Grant-in-Aid for Scientific Research (B) from the Ministry of Education, Science, Sports and Culture of Japan.

References

[1] I. Angulo, J. Rullas, J.A. Campillo, E. Obregon, A. Heath, M. Howard, M.A. Munoz-Fernandez, J.L. Subiza, Early myeloid cells are high producers of nitric oxide upon CD40 plus IFN-gamma stimulation through a mechanism dependent on endogenous TNF-alpha and IL-1alpha, Eur. J. Immunol. 30 (2000) 1263–1271.

[2] R. Bischoff, Proliferation of muscle satellite cells on intact myofibers in culture, Dev. Biol. 115 (1986) 129–139.

[3] R. Bischoff, The satellite cell and muscle regeneration, in: A.G. Myology, C. Engel, A. Franszini-Armstrong (Eds.), McGraw-Hill, New York, 1994, pp. 97–118.

[4] R.E. Bittner, C. Schöfer, K. Weipoltshammer, S. Ivanova, B. Streubel, E. Hauser, M. Freilinger, H. Höger, A. Elbe-Bürger, F. Wachtler, Recruitment of bone-marrow-derived cells by skeletal muscle and cardiac muscle in adult dystrophic mdx mice, Anat. Embryol. 199 (1999) 391–396.

[5] T.R. Brazelton, M. Nystrom, H.M. Blau, Significant differences among skeletal muscles in the incorporation of bone marrow-derived cells, Dev. Biol. 262 (2003) 64–74.

[6] F.D. Camargo, R. Green, Y. Capetenoki, K.A. Jackson, M.A. Goodell, Single hematopoietic stem cells generate skeletal muscle through myeloid intermediates, Nat. Med. 9 (2003) 1520–1527.

[7] R.F. Castro, K.A. Jackson, M.A. Goodell, C.S. Robertson, H. Liu, H.D. Shine, Failure of bone marrow cells to transdifferentiate into neural cells in vivo, Science 297 (2002) 1299.

[8] S.Y. Corbel, A. Lee, J. Duenas, T.R. Brazelton, H.M. Blau, F.M. Rossi, Contribution of hematopoietic stem cells to skeletal muscle, Nat. Med. 9 (2003) 1528–1532.

[9] R. Couteaux, J.-C. Mira, A. d'Albis, Regeneration of muscles after cardiotoxin injury. I. Cytological aspects, Biol. Cell 62 (1988) 171–182.

[10] L.D. De Angelis, L. Berghella, M. Coletta, L. Lattanzi, M. Zanchi, M.G.C. De Angelis, C. Ponzetto, G. Cossu, Skeletal myogenic progenitors originating from embryonic dorsal aorta coexpress endothelial and myogenic markers and contribute to postnatal muscle growth and regeneration, J. Cell Biol. 147 (1999) 869–877.

[11] C.D. De Bari, F. Dell'Accio, F. Vandenabeele, J.R. Vermeesch, J.-M. Raymackers, F.P. Luyten, Skeletal muscle repair by adult human mesenchymal stem cells from synovial membrane, J. Cell Biol. 160 (2003) 909–918.

[12] G. Ferrari, M.G.C. De Angelis, M. Coletta, E. Paolucci, A. Stornaiuolo, G. Cossu, F. Mavilio, Muscle regeneration by bone marrow-derived myogenic progenitors, Science 279 (1998) 1528–1530.

[13] G. Ferrari, A. Stornaiuolo, F. Mavilio, Failure to correct murine muscular dystrophy, Nature 411 (2001) 1014–1015.

[14] J.E. Fletcher, M.-S. Jiang, Possible mechanisms of action of cobra snake venom cardiotoxins and bee venom melittin, Toxicon 31 (1993) 669–695.

[15] S. Fukada, Y. Miyagoe-Suzuki, H. Tsukihara, K. Yuasa, S. Higuchi, S. Ono, K. Tsujikawa, S. Takeda, H. Yamamoto, Muscle regeneration by reconstitution with bone marrow or fetal liver cells from green fluorescent protein-gene mice, J. Cell Sci. 115 (2002) 1285–1293.

[16] M.A. Goodell, K. Brose, G. Paradis, A.S. Conner, R.C. Mulligan, Isolation and functional properties of murine hematopoietic stem cells that are replicating in vitro, J. Exp. Med. 183 (1996) 1797–1806.

[17] M.A. Goodell, M. Rosenzweig, H. Kim, D.F. Marks, M. DeMaria, G. Paradis, S.A. Grupp, C.A. Sieff, R.C. Mulligan, R.P. Johnson, Dye efflux studies suggest that hematopoietic stem cells expressing low or undetectable levels of CD34 antigen exist in multiple species, Nat. Med. 3 (1997) 1337–1345.

[18] E. Gussoni, Y. Soneoka, C.D. Strickland, E.A. Buzney, M.K. Khan, A.F. Flint, L.M. Kunkel, R.C. Mulligan, Dystrophin expression in the mdx mouse restored by stem cell transplantation, Nature 401 (1999) 390–394.

[19] A. Hirata, S. Masuda, T. Tamura, K. Kai, K. Ojima, A. Fukase, K. Motoyoshi, K. Kamakura, Y. Miyagoe-Suzuki, S. Takeda, Expression profiling of cytokines and related genes in regenerating skeletal muscle after cardiotoxin injection: a role for osteopontin, Am. J. Pathol. 163 (2003) 203–215.

[20] K.A. Jackson, T. Mi, M. Goodell, Hematopoietic potential of stem cells isolated from murine skeletal muscle, Proc. Natl. Acad. Sci. USA 96 (1999) 14482–14486.

[21] H. Kawada, M. Ogawa, Bone marrow origin of hematopoietic progenitors and stem cells in murine muscle, Blood 98 (2001) 2008–2013.

[22] M.A. LaBarge, H.M. Blau, Biological progression from adult bone marrow to mononucleate muscle stem cell to multinucleate muscle fiber in response to injury, Cell 111 (2002) 589–601.

[23] S.L. McKinney-Freeman, S.M. Majka, K.A. Jackson, K. Norwood, K.K. Hirschi, M.A. Goodell, Altered phenotype and reduced function of muscle-derived hematopoietic stem cells, Exp. Hematol. 31 (2003) 806–814.

[24] F. Montanaro, K. Liadaki, J. Volinski, A. Flint, L.M. Kunkel, Skeletal muscle engraftment potential of adult mouse skin side population cells, Proc. Natl. Acad. Sci. USA 100 (2003) 9336–9341.

[25] A. Musarò, C. Giacinti, G. Borsellino, G. Dobrowolny, L. Pelosi, L. Cairns, S. Ottolenghi, G. Cossu, G. Bernardi, L. Battistini, M. Molinaro, N. Rosenthal, Stem cell-mediated muscle regeneration is enhanced by local isoform of insulin-like growth factor 1, Proc. Natl. Acad. Sci. USA 101 (2004) 1206–1210.

[26] M. Ogawa, Y. Matsuzaki, S. Nishikawa, S. Hayashi, T. Kunisada, T. Sudo, T. Kina, H. Nakauchi, S. Nishikawa, Expression and function of c-kit in hemopoietic progenitor cells, J. Exp. Med. 174 (1991) 63–71.

[27] M. Okabe, M. Ikawa, K. Kominami, T. Nakanishi, Y. Nishimune, 'Green mice' as a source of ubiquitous green cells, FEBS Lett. 407 (1997) 313–319.
[28] D.J. Pearce, C.M. Ridler, C. Simpson, D. Bonnet, Multi-parameter analysis of murine bone marrow side population cells, Blood (2003).
[29] P. Ralph, M.-K. Ho, P.B. Litcofsky, T.A. Springer, Expression and induction in vitro of macrophage differentiation antigens on murine cell lines, J. Immunol. 130 (1983) 108–114.
[30] T. Reya, N.V. Contractor, M.S. Couzens, M.A. Wasik, S.G. Emerson, S.R. Carding, Abnormal myelocytic cell development in interleukin-2 (IL-2)-deficient mice: evidence for the involvement of IL-2 in myelopoiesis, Blood 91 (1998) 2935–2947.
[31] J.D. Rosenblatt, A.I. Lunt, D.J. Parry, T.A. Partridge, Culturing satellite cells from living single muscle fiber explants, In Vitro Cell. Dev. Biol.-Animal. 31 (1995) 773–779.
[32] C.W. Scharenberg, M.A. Harkey, B. Torok-Storb, The ABCG2 transporter is an efficient Hoechst 33342 efflux pump and is preferentially expressed by immature human hematopoietic progenitors, Blood 99 (2002) 507–512.
[33] P. Seale, M.A. Rudnicki, A new look at the origin, function, and stem-cell status of muscle satellite cells, Dev. Biol. 218 (2000) 115–124.
[34] I.S. Trowbridge, M.L. Thomas, CD45: an emerging role as a protein tyrosine phosphatase required for lymphocyte activation and development, Annu. Rev. Immunol. 12 (1994) 85–116.
[35] S. Wakitani, T. Saito, A.I. Caplan, Myogenic cells derived from rat bone marrow mesenchymal stem cells exposed to 5-azacytidine, Muscle Nerve 18 (1995) 1417–1426.
[36] M. Ye, H. Iwasaki, C.V. Laiosa, M. Stadtfeld, H. Xie, S. Heck, B. Clausen, K. Akashi, T. Graf, Hematopoietic stem cells expressing the myeloid lysozyme gene retain long-term, multilineage repopulation potential, Immunity 19 (2003) 689–699.
[37] B.P. Zambrowicz, A. Imamoto, S. Fiering, L.A. Herzenberg, W.G. Kerr, P. Soriano, Disruption of overlapping transcripts in the ROSA βgeo 26 gene trap strain leads to widespread expression of β-galactosidase in mouse embryos and hematopoietic cells, Proc. Natl. Acad. Sci. USA 94 (1997) 3489–3794.
[38] P.S. Zammit, L. Heslop, V. Hudon, J.D. Rosenblatt, S. Tajbakhsh, M.E. Buckingham, J.R. Beauchamp, T.A. Partridge, Kinetics of myoblast proliferation show that resident satellite cells are competent to fully regenerate skeletal muscle fibers, Exp. Cell Res. 281 (2002) 39–49.
[39] Y. Zhao, D. Glesne, E. Huberman, A human peripheral blood monocyte-derived subset acts as pluripotent stem cells, Proc. Natl. Acad. Sci. USA 100 (2003) 2426–2431.

Human Molecular Genetics, 2004, Vol. 13, No. 16 *1775–1784*
doi:10.1093/hmg/ddh190
Advance Access published on June 22, 2004

Laminin α1 chain reduces muscular dystrophy in laminin α2 chain deficient mice

Kinga Gawlik[1], Yuko Miyagoe-Suzuki[2], Peter Ekblom[1], Shin'ichi Takeda[2] and Madeleine Durbeej[1,*]

[1]Department of Cell and Molecular Biology, Section for Cell and Developmental Biology, University of Lund, Lund, Sweden and [2]Department of Molecular Therapy, National Institute of Neuroscience, National Center of Neurology and Psychiatry, Kodaira, Tokyo, Japan

Received April 14, 2004; Revised and Accepted June 11, 2004

Laminin (LN) α2 chain deficiency in humans and mice leads to severe forms of congenital muscular dystrophy (CMD). Here, we investigated whether LNα1 chain in mice can compensate for the absence of LNα2 chain and prevent the development of muscular dystrophy. We generated mice expressing a LNα1 chain transgene in skeletal muscle of LNα2 chain deficient mice. LNα1 is not normally expressed in muscle, but the transgenically produced LNα1 chain was incorporated into muscle basement membranes, and normalized the compensatory changes of expression of certain other laminin chains (α4, β2). In 4-month-old mice, LNα1 chain could fully prevent the development of muscular dystrophy in several muscles, and partially in others. The LNα1 chain transgene not only reversed the appearance of histopathological features of the disease to a remarkable degree, but also greatly improved health and longevity of the mice. Correction of LNα2 chain deficiency by LNα1 chain may serve as a paradigm for gene therapy of CMD in patients.

INTRODUCTION

Laminins (LN), major components of basement membranes, are heterotrimers of α-, β- and γ-chains. The five α-, three β- and three γ-chains give rise to at least 15 different protein isoforms that differ in their tissue distribution (1,2). Mutations in the *LAMA2* gene encoding the LNα2 chain—the main α chain in skeletal muscle—cause congenital muscular dystrophy (CMD) with LNα2 chain deficiency. In European populations this accounts for about 50% of the classical CMDs (3). This disorder shows autosomal recessive inheritance and is characterized by neonatal onset of muscle weakness, hypotonia, early muscle fiber degeneration and white matter abnormalities (4–6).

Two knock-out mouse models (dy^w/dy^w, dy^{3K}/dy^{3K}) and three spontaneous mutant mouse strains (dy/dy, dy^{2J}/dy^{2J}, dy^{Pas}/dy^{Pas}) representing animal models for CMD with LNα2 chain deficiency have been reported (7–12). The dy^w/dy^w mice still express small amounts of a truncated LNα2 chain, whereas the dy^{3K}/dy^{3K} mice are completely deficient in LNα2 chain. Both strains develop early and severe clinical signs of muscular dystrophy (7–9). In addition, LNα2 chain deficiency in mice results in defects in multiple tissues including peripheral and central nervous systems (7,8,13–15).

The development of therapies for muscular dystrophy involves *in vivo* strategies aiming to introduce a normal copy of the defective gene (16). Indeed, it has been demonstrated that a human LNα2 chain transgene can rescue the dystrophic symptoms in the dy^w/dy^w mouse (8). However, one major obstacle of gene transfer is the tendency of the immune system to reject novel antigens (16). Instead, delivery of homologous genes already expressed at other sites in the body could eradicate these concerns. Utrophin can compensate for dystrophin deficiency and prevent the development of muscular dystrophy in a mouse model for Duchenne muscular dystrophy (17). Yet, there is no evidence that homologous gene therapy would work in CMD.

In several mouse models for LN deficiency other LN chains are upregulated. The LNα4 chain is upregulated in the LNα2 chain deficient muscle, but this upregulation is inadequate to prevent muscular dystrophy (18). Similarly, the upregulation of LNβ1 chain in the glomerular basement membrane of LNβ2 chain deficient kidneys does not prevent nephrosis (19). In addition, some basement membranes in LNα5 chain deficient mice are ultrastructurally defective despite ectopic

*To whom correspondence should be addressed at: Department of Cell and Molecular Biology, Section for Cell and Developmental Biology, University of Lund, BMC B12, 221 84 Lund, Sweden. Tel: +46 462220812; Fax: +46 462220855; Email: madeleine.durbeej_hjalt@medkem.lu.se

deposition of other α-chains (20). Thus, whether LN chains functionally can compensate for each other *in vivo* remains to be determined.

Here, we analyzed whether LNα1 chain, which is mainly expressed in epithelial cells (21,22), could compensate for LNα2 chain deficiency and rescue the dystrophic symptoms in LNα2 chain deficient dy^{3K}/dy^{3K} mice. LNα1 chain was chosen as a therapeutic protein, because this α-chain is structurally most similar to LNα2 chain (1,23). Furthermore, LN-1, which contains the α1-chain, can significantly promote myogenesis *in vitro* (24), perhaps by binding to integrins (25) or dystroglycan (26). Yet, there are also notable differences between the LNα1 and LNα2 chains. The α2-chain binds much more efficiently to dystroglycan than the α1-chain (26). Myoblast spreading is significantly faster on α2LNs than on α1LNs (27), and α2LNs have been reported to be specifically required for myotube stability and survival *in vitro* (28). Therefore, it was by no means clear from previous studies that LNα1 chain would compensate for lack of α2-chain in muscles *in vivo*.

We demonstrate that expression of LNα1 chain transgene in skeletal muscles of dy^{3K}/dy^{3K} mice reduces the dystrophy symptoms in these animals as evaluated by histology of muscle, weight gain and longevity of the animals. Our data also illustrate for the first time that LNα chains can functionally compensate for each other *in vivo*.

RESULTS

Generation and characterization of LNα1 chain transgenic mice

LNα1 chain is mainly limited to some epithelial basement membranes in adult mice (21). To achieve broad expression of LNα1 chain as a transgene, the cDNA for mouse LNα1 chain was inserted into a vector driven by the cytomegalovirus (CMV) enhancer and the chicken β-actin promoter, followed by the rabbit β-globin polyadenylation signal (29) (Fig. 1A). Fifty-one mice were born from microinjected fertilized eggs. Thirteen of the mice carried the transgene as detected by Southern blot analyses (data not shown). Our primary goal was to study the effects of the LNα1 transgene in LNα2 chain deficient muscle. Thus, we selected mice expressing LNα1 chain in skeletal muscle. Five of the 13 mice showed immunofluorescence staining of LNα1 chain to a varying degree in skeletal muscles. Skeletal muscles from line No. 12 contained high expression of LNα1 chain, and were selected for further analysis and for production of dy^{3K} mice lacking LNα2 chain but expressing LNα1 chain. The data presented were obtained with mice derived from line No. 12. Reverse transcription–polymerase chain reaction (RT–PCR) reactions yielded a 532 bp amplicon corresponding to a LNα1 chain product in transgenic mice (Fig. 1B). No LNα1 chain was detected in skeletal muscle of wild-type mice (Fig. 1C–E) (30). In contrast, immunofluorescence staining demonstrated the presence of LNα1 chain in basement membranes of skeletal and cardiac muscle in line No. 12 (Fig. 1C). Also, blood vessels within muscle, which normally do not express LNα1 chain (21), were positively stained for LNα1 chain (Fig. 1C). In skeletal muscle, LNα1 chain was also detected in the neuromuscular and myotendinous junctions (Fig. 1D and E). LNα1 chain expression was noted in other organs (e.g. salivary gland, pancreas and thymus) where it is normally not expressed (data not shown). However, LNα1 chain was not present in the sciatic nerve of line No. 12 (Fig. 1C). Importantly, overexpression of LNα1 chain in mice revealed no discernible pathological phenotypes.

We next produced mice heterozygous for the transgene and homozygous for the dy^{3K} mutation, hereafter called dy^{3K}LNα1TG. The LNα1 transgene was expressed in these mice in the same manner as the transgenic line No. 12 (Fig. 3).

Dy^{3K}/dy^{3K} mice with LNα1 transgene are healthy and long-lived

Dy^{3K}/dy^{3K} mice are characterized by growth retardation and severe muscular dystrophy symptoms (7). As shown in Figure 2A and B, the overall health of dy^{3K}LNα1TG mice was significantly improved compared with dy^{3K}/dy^{3K} mice. First, dy^{3K}LNα1TG mice are bigger than dy^{3K}/dy^{3K} mice. At 2 weeks of age, dy^{3K}/dy^{3K} mice can be identified owing to their growth retardation, whereas dy^{3K}LNα1TG mice appeared outwardly normal (data not shown). Weight gain for dy^{3K}/dy^{3K} mice was greatly delayed in 5-week-old mice, whereas the weight gain for dy^{3K}LNα1TG mice was significantly increased compared with dy^{3K}/dy^{3K} mice (Fig. 2C). In addition, the average body weight of 10-week-old dy^{3K}LNα1TG mice was close to that of wild-type mice (Fig. 2D). Second, dy^{3K}LNα1TG mice live longer. On an average, dy^{3K}/dy^{3K} mice died at the age of 4–5 weeks (Fig. 2E). Besides the death of a single dy^{3K}LNα1TG mouse, dy^{3K}LNα1TG mice survived beyond 10 weeks (Fig. 2E). Currently, our oldest mouse is 11 months old.

Previous studies have shown that 4-week-old LNα2 chain deficient mice display a significantly reduced locomotory activity (31). Here, we analyzed the activity of older dy^{3K}LNα1TG mice (10–17-week-old). Exploratory locomotion studies revealed that dy^{3K}LNα1TG mice appeared as active as wild-type mice (Fig. 2F). An additional indication for the improved health is that both male and female dy^{3K}LNα1TG mice are able to produce offspring (data not shown). Dy^{3K}/dy^{3K} mice die before reaching reproductive age, however, *dy/dy* mice survive longer but do not reproduce (32) (www.jax.org).

Localization of basement membrane components in muscles of dy^{3K}LNα1TG mice

As expected, LNα2 chain was completely absent in dy^{3K}LNα1TG mice (Fig. 3). In wild-type mice, LNα4 and LNα5 chains were mainly expressed in blood vessels. In agreement with previous studies, the expression of the LNα4 chain was strongly increased at the muscle basement membrane area in dy^{3K}/dy^{3K} mice, whereas the LNα5 chain was weakly upregulated (18,31) (Fig. 3). In dy^{3K}LNα1TG mice, the muscle basement membrane expression of LNα4 chain was down-regulated to some extent, whereas the expression of LNα5 chain remained unchanged. Cohn *et al.* (33) have previously reported a reduction of LNβ2 staining in skeletal muscle membranes of CMD patients with LNα2 deficiency.

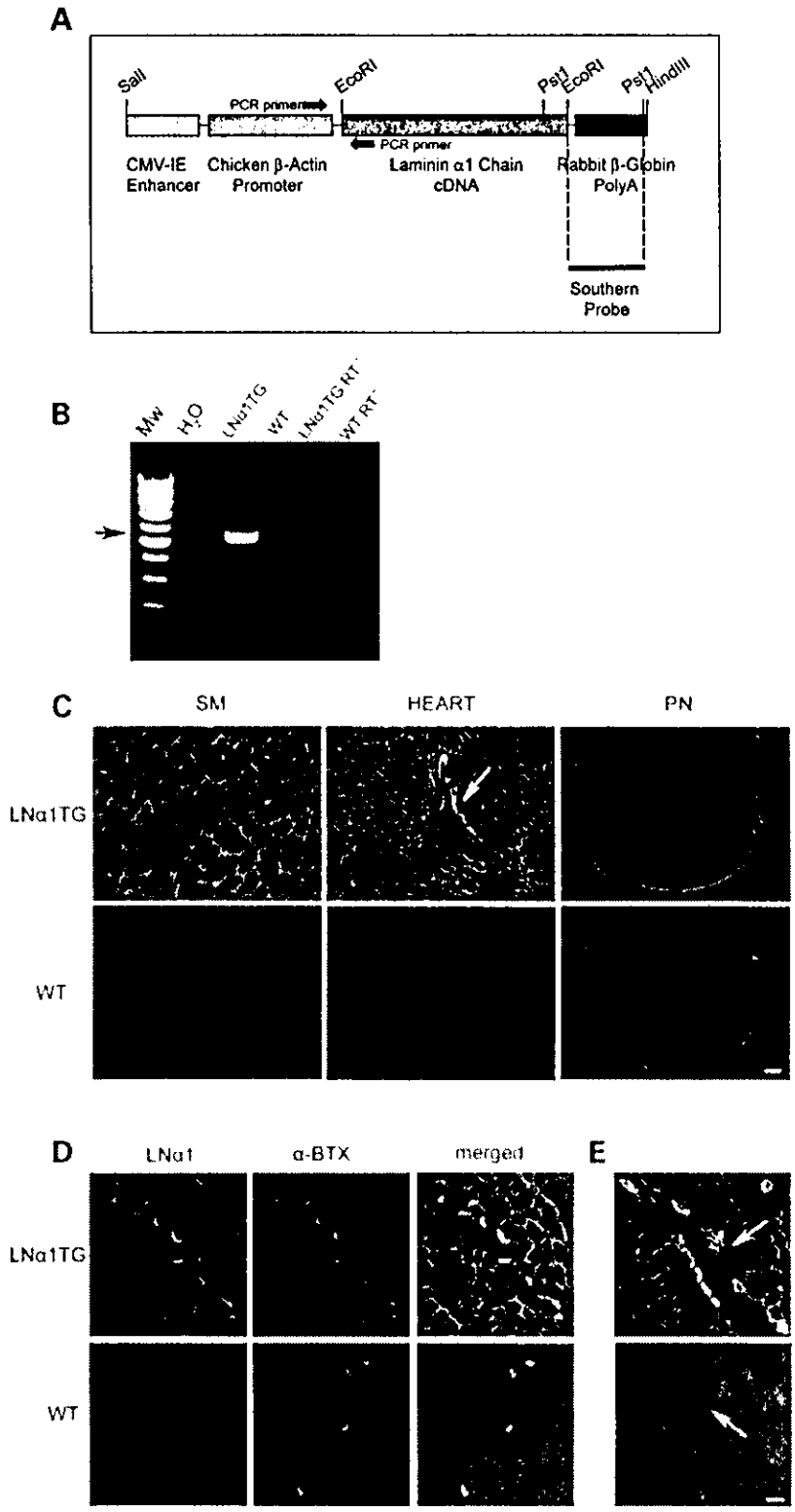

Figure 1. Overexpression of LNα1 chain in transgenic mice. **(A)** cDNA encoding LNα1 chain was subcloned into the pCAGGS expression vector. Restriction sites used to engineer the construct are shown. **(B)** PCR amplification of reverse transcribed mRNA from transgenic (LNα1TG) and wild-type (WT) skeletal muscle. **(C)** Expression of LNα1 chain in transgenic mice from the No. 12 line. LNα1 chain was expressed in the skeletal muscle (SM) (tibialis anterior) and the heart, but not in the peripheral nerve (PN) of transgenic mice or in the corresponding wild-type tissues. The arrow denotes a LNα1 chain positively stained blood vessel. **(D)** Localization of LNα1 chain in neuromuscular junction. Sections from skeletal muscle containing neuromuscular junctions of LNα1 chain transgenic and wild-type mice were doubly stained with antibodies against LNα1 chain (red) and fluorescein α-bungarotoxin (α-BTX, green). **(E)** Localization of LNα1 chain at the myotendinous junction (arrows). Bar, 50 μm.

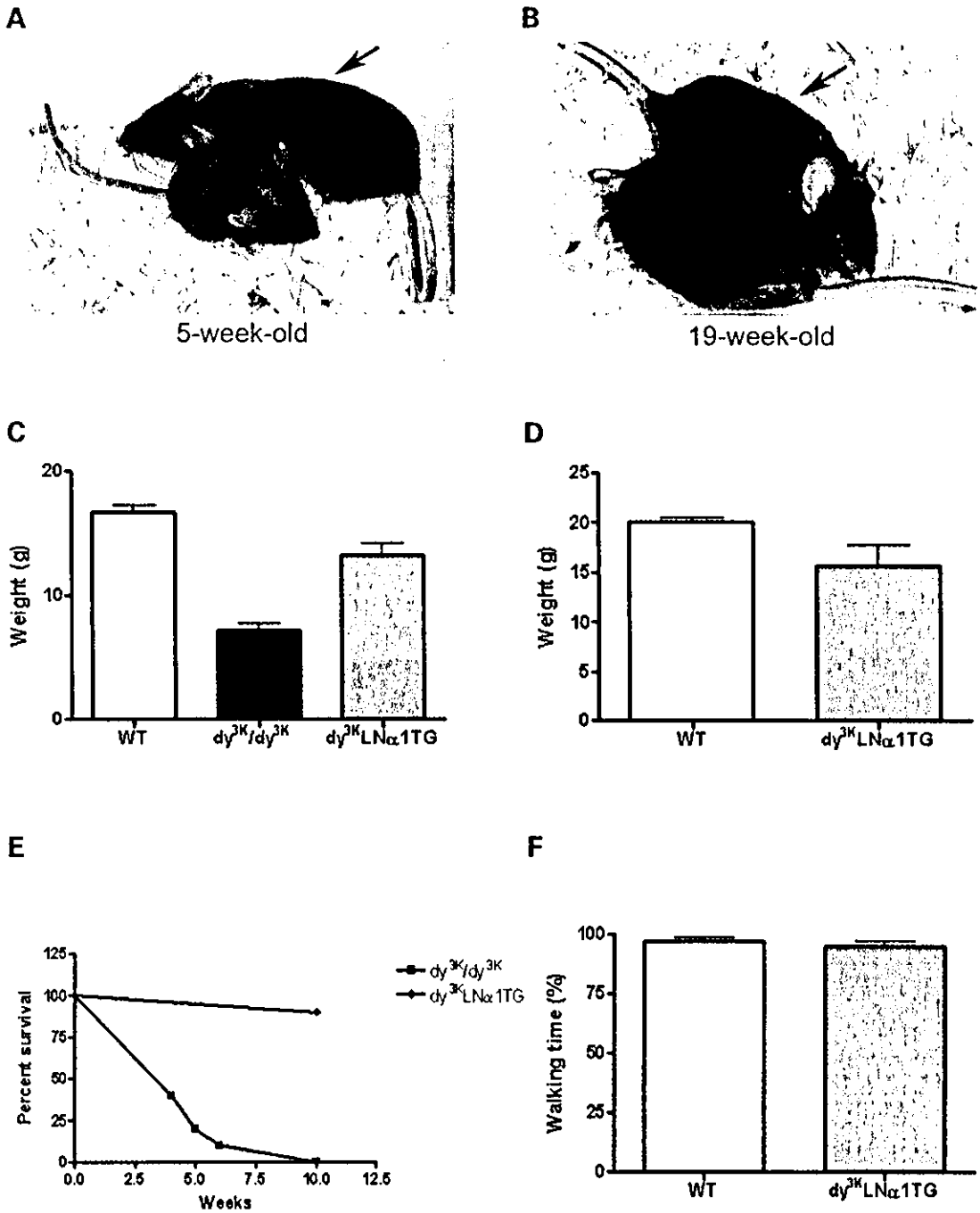

Figure 2. Overall phenotype of LNα2 chain deficient animals expressing the LNα1 chain transgene. **(A)** The 5-week-old dy^{3K}LNα1TG mice (arrow) are larger than the emaciated dy^{3K}/dy^{3K} mice. **(B)** The 5-month-old dy^{3K}LNα1TG mice (arrow) remain alert and lively with good muscle tone. A dy^{3K}LNα1TG littermate is shown for comparison. **(C)** Whole body weights of 5-week-old female wild-type, dy^{3K}/dy^{3K} and dy^{3K}LNα1TG mice. Each bar represents the mean ± SEM of six (WT), four (dy^{3K}/dy^{3K}) and five (dy^{3K}LNα1TG) mice. Note that dy^{3K}LNα1TG mice weigh significantly more than dy^{3K}/dy^{3K} mice ($P < 0.001$). **(D)** Whole body weights of 10-week-old female wild-type and dy^{3K}LNα1TG mice. Each bar represents the mean ± SEM of six (WT) and five (dy^{3K}LNα1TG) mice ($P > 0.05$). **(E)** Survival curves of dy^{3K}/dy^{3K} ($n = 10$) and dy^{3K}LNα1TG mice ($n = 10$). One death occurred in the group of dy^{3K}LNα1TG mice (at the age of 10 weeks), whereas most of the dy^{3K}/dy^{3K} mice died between 4 and 5 weeks. **(F)** Exploratory locomotion of 10–17-week-old female mice in an open field test. Each value represents the mean ± SEM of 4 mice.

Similarly, we noted a moderate reduction of LNβ2 chain in dy^{3K}/dy^{3K} mice. Interestingly, the expression of LNβ2 chain in the skeletal muscle membrane of dy^{3K}LNα1TG mice was also normalized to expression levels seen in wild-type mice (Fig. 3). Other basement membrane components including type IV collagen and perlecan were similarly expressed in wild-type, dy^{3K}/dy^{3K} and in dy^{3K}LNα1TG mice (Fig. 3). Dystroglycan (composed of α- and β-subunits) is a major receptor

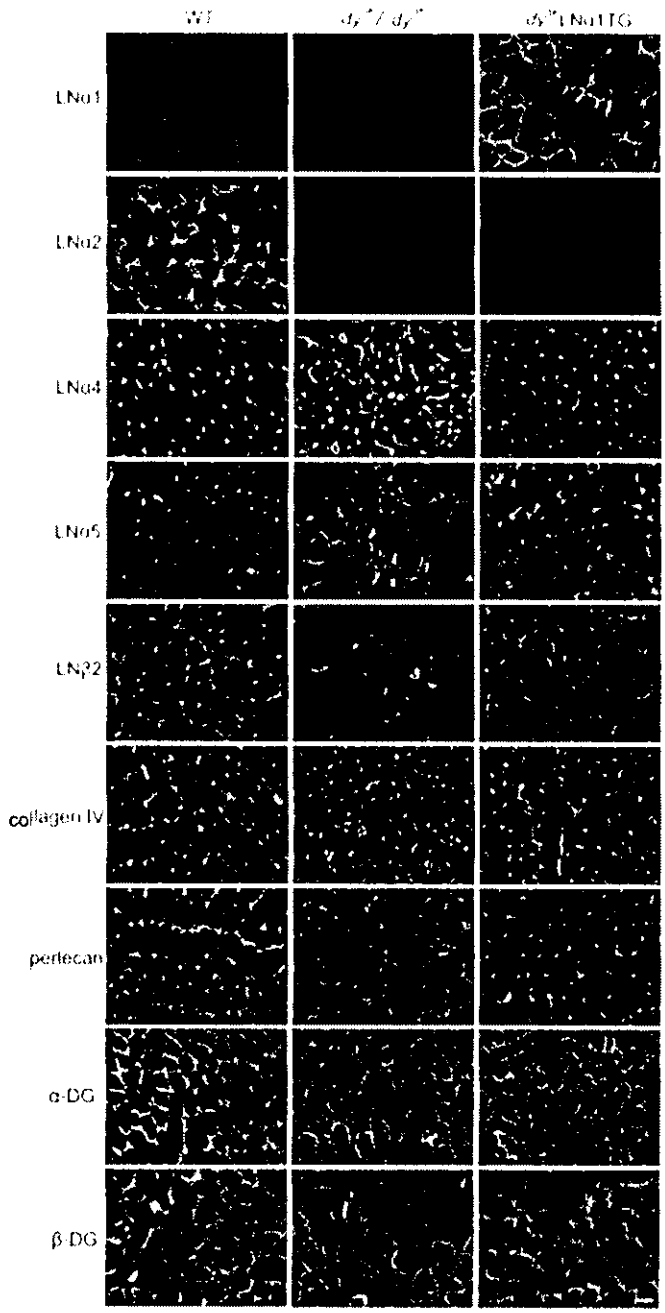

Figure 3. Immunostaining of LNs, perlecan, collagen IV and dystroglycan. Cross-sections of skeletal muscles (tibialis anterior) from 2-week-old wild-type, dy^{3K}/dy^{3K} and dy^{3K}LNα1TG mice were stained with antibodies against LNα1, LNα2, LNα4, LNα5 and LNβ2 chains; perlecan; collagen IV; α-dystroglycan and β-dystroglycan. Bar, 50 μm.

for several LNs (26,34). It was recently suggested on the basis of immunofluorescence that the amount of α-dystroglycan is decreased, whereas the expression of β-dystroglycan is increased in dy^W/dy^W mice compared with controls (31). Yet, using similar assays but different antibodies, we found no differences in the expression patterns of α- or β-dystroglycan between normal mice and dy^{3K}/dy^{3K} or dy^{3K}LNα1TG mice (Fig. 3).

LNα1 transgene reduces dystrophic pathology of skeletal muscles

We next examined the morphology of dy^{3K}/dy^{3K} and dy^{3K}LNα1TG skeletal muscle. Histological features of dystrophic muscle in 2-week-old dy^{3K}/dy^{3K} mice included large groups of centrally nucleated small-caliber muscle fibers revealing the process of active regeneration (7). In contrast, muscles from 2-week-old dy^{3K}LNα1TG mice had a near normal morphology with significantly fewer central nuclei (Fig. 4A and B). Hence, LNα1 chain expression protected myofibers from degeneration. In 2-week-old dy^{3K}/dy^{3K} mice there was a nearly complete absence of basement membrane around muscle fibers as revealed by electron microscopy studies (Fig. 4C) (7). The LNα1 chain transgene restored the basement membrane in dy^{3K}LNα1TG mice (Fig. 4C).

To investigate whether the LNα1 chain also prevented pathological changes in older mice we analyzed skeletal muscles (quadriceps femoris, gluteus maximus, tibialis anterior, triceps brachii and diaphragm) from 4-month-old mice. No dy^{3K}/dy^{3K} mice survive till that age. Skeletal muscles of 3–4-week-old dy^{3K}/dy^{3K} mice display signs of a severe dystrophy with pronounced fibrosis characteristic of LNα2 chain deficient CMD (Fig. 5) (7). In addition, *dy/dy* mice show extensive fibrosis in various muscles (35). Fibrous tissue is believed to replace muscle when the myogenic satellite cell pool becomes exhausted and consequently fail to maintain muscle regeneration (36). Noticeably, no pathological fibrous tissue was detected in skeletal muscles of 4-month-old dy^{3K}LNα1TG mice (Fig. 5), whereas pronounced fibrosis was detected in all muscles of 3.5-week-old dy^{3K}/dy^{3K} mice (Fig. 5). In quadriceps femoris of dy^{3K}LNα1TG mice most fibers were of polygonal shape and normal size, and very few fibers had internally placed nuclei (Fig. 5). A very mild myopathy was detected in gluteus maximus of dy^{3K}LNα1TG mice, with occasional areas of fibers with centrally located nuclei (Fig. 5). In tibialis anterior and triceps brachii of dy^{3K}LNα1TG mice we noted larger areas with centrally located nuclei but no fibrosis (Fig. 5). In contrast, diaphragm of dy^{3K}LNα1TG mice had a near normal morphology with no fibrosis, regular myofibre size and virtually no centralized nuclei, whereas severe fibrosis was detected in diaphragm of dy^{3K}/dy^{3K} mice (Fig. 5).

In mature *dy/dy* muscle, the expression of tenascin-C is upregulated and extended to the interstitium between muscle fibers, especially within focal lesions, whereas in control muscle, tenascin-C expression is restricted to the myotendinous junction (37). In sharp contrast to this, very little tenascin-C expression was noted in skeletal muscles of dy^{3K}LNα1TG mice (Fig. 6 and data not shown).

LNα2 chain deficiency also results in dysmyelination of peripheral nerve (38–40), a phenotype that was not corrected in dy^{3K}LNα1TG mice, as the LNα1 chain was not expressed in peripheral nerve (Fig. 1C). Injury to peripheral nerve causes neurogenic atrophy of muscle fibers. Accordingly, we noted occasional shrunken angular muscle fibers indicating neurogenic lesions in several muscles of 4-month-old dy^{3K}LNα1TG mice (Fig. 7).

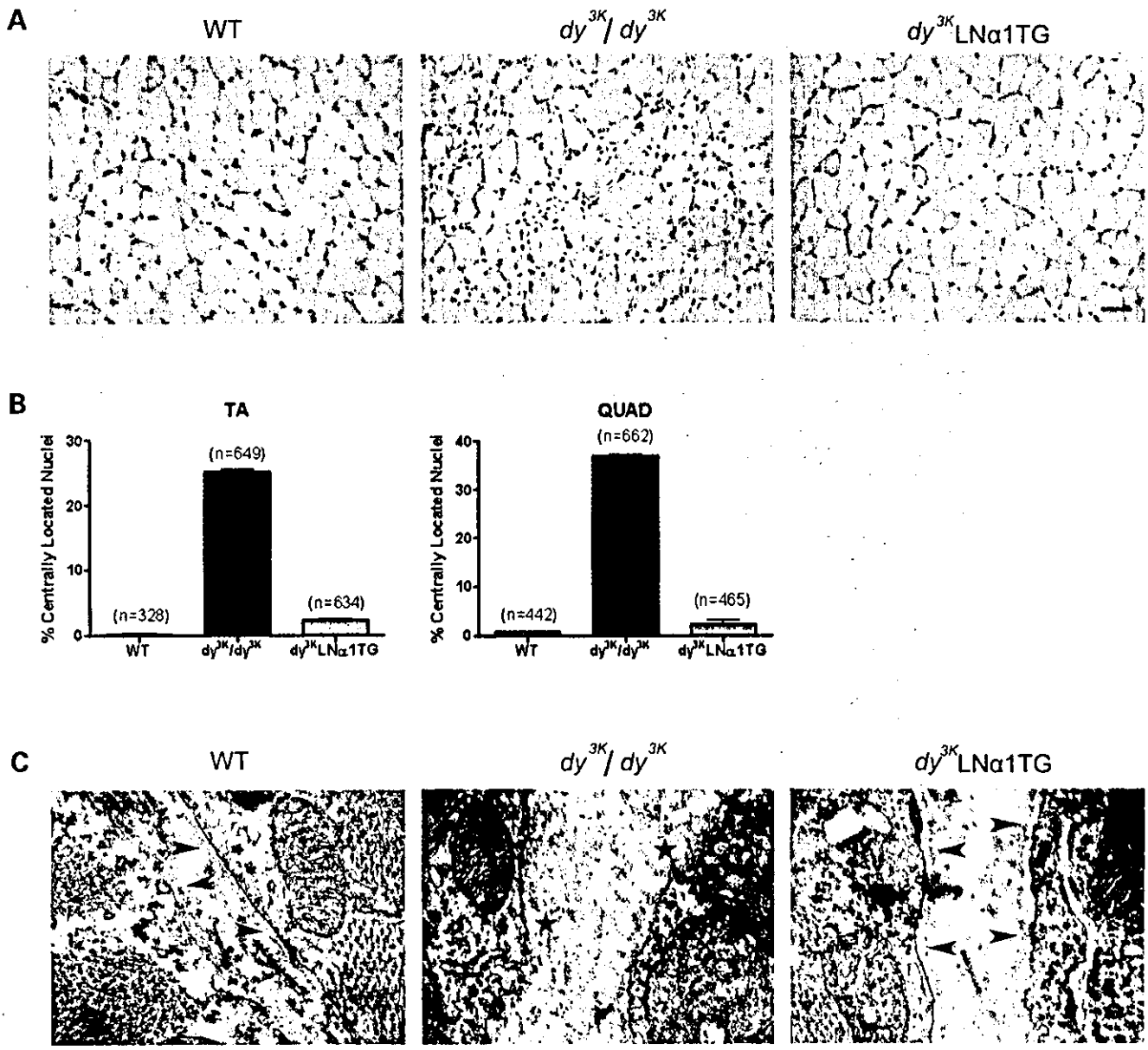

Figure 4. Analyses of skeletal muscles from different mice. (A) H&E staining of tibialis anterior muscles of 2-week-old wild-type, dy^{3K}/dy^{3K} and dy^{3K}LNα1TG mice. Dystrophic changes with large groups of centrally nucleated small-caliber muscle fibers were detected in dy^{3K}/dy^{3K} mice. Muscle degeneration was prevented in dy^{3K}LNα1TG mice. Bar, 50 μm. (B) Quantification of central nucleation in tibialis anterior (TA) and quadriceps femoris (QUAD) muscles from 2-week-old mice. The number of fibers examined for each sample is given in parenthesis. (C) Transmission electron microscopy of tibialis anterior muscle. The basement membrane, clearly present along the sarcolemma in wild-type mouse, was almost absent in muscle fibers of 2-week-old dy^{3K}/dy^{3K} mice (indicated by asterisks). The basement membrane (arrows) was restored in dy^{3K}LNα1TG mice. Bar, 300 nm.

DISCUSSION

We report that LNα2 chain deficient mice expressing a LNα1 chain transgene in skeletal muscle display a prolonged life, better health and improved muscle morphology. The greatly improved health of the LNα2 chain deficient mice induced by the transgene was remarkable for several reasons. First, although some classical studies showed that the LNα1 chain can promote short-term myogenesis *in vitro* (24,41), α2 chain LNs are much better than α1 chain LNs as *in vitro* stimulators of myoblast spreading (27) and myotube stability and survival (28). Second, detailed studies of LN receptors have revealed that LNα1 chain binds to dystroglycan with about 10-fold lower affinity than LNα2 chain or agrin (26), and dystroglycan is an essential link between the extracellular matrix and the cytoskeleton in muscle (42). Third, compensatory upregulation of other LN chains in mouse knock-out models of other LN chains appears to be of no apparent help (1).

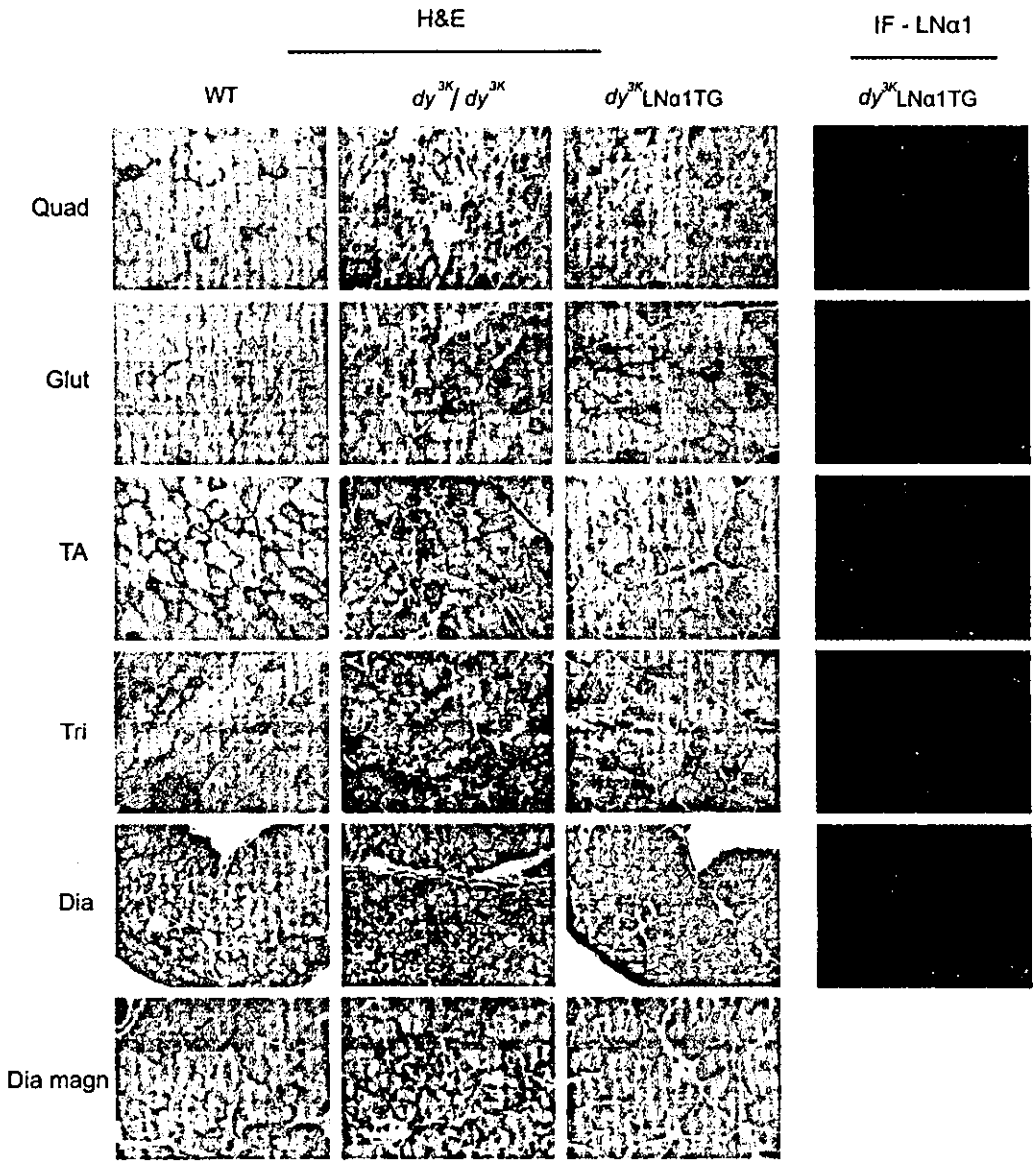

Figure 5. H&E staining of various muscles from 4-month-old wild-type mice, 3.5-week-old dy^{3K}/dy^{3K} mice and 4-month-old dy^{3K}LNα1TG mice. Cryosections of quadriceps femoris (Quad), gluteus maximus (Glut), tibialis anterior (TA), triceps brachii (Tri) and diaphragm (Dia) were stained with H&E and with antibodies against LNα1 chain (staining in red in the last column). Dia magn. represents higher magnification of diaphragm. Bar, 50 μm.

Recently, it was reported that an agrin minigene similarly can rescue dystrophic symptoms in the dy^{W}/dy^{W} mouse model of CMD. In these experiments, LNα5 chain expression was significantly enhanced, suggesting an indirect mechanism of rescue (31). No enhanced expression of LNα5 chain was seen in the present study. Hence, we consider it likely that the neo-expression of LNα1 in muscles is the major cause of the rescue, although we cannot exclude that expression in other tissues also was beneficial.

Our results indicate that early gene transfer of LNα1 chain into skeletal muscles constitute promising therapeutic strategies for LNα2 chain deficient CMD. This could be achieved by introducing LNα1 chain into myofibers by the usage of viral vectors. Because the LNα1 chain cDNA is fairly large (~9 kb), gutted adenoviral vectors, which have a cloning capacity > 30 kb, would be the viral vector of choice (43). Investigations aiming at up-regulating endogenous LNα1 chain in skeletal muscle are also merited. For example, constitutively active Akt-1 induces transcription and synthesis of LNα1 chain in embryonic stem cells (44). However, Akt controls numerous transcription factors and is considered to be a hot drug target for the treatment of cancer, diabetes and stroke (45). Thus, it is unlikely to be specific for the treatment of CMD. Interestingly, the identification of an upstream enhancer in the mouse LNα1 chain was recently reported (46). This enhancer activates LNα1 chain expression in parietal endoderm cells, and activating this enhancer in muscle cells could be a possible strategy in the treatment of LNα2 chain deficient CMD.

Peripheral nerve is also involved in LNα2 chain deficient CMD (6,38–40). In addition, dy^{3K}LNα1TG mice flexed

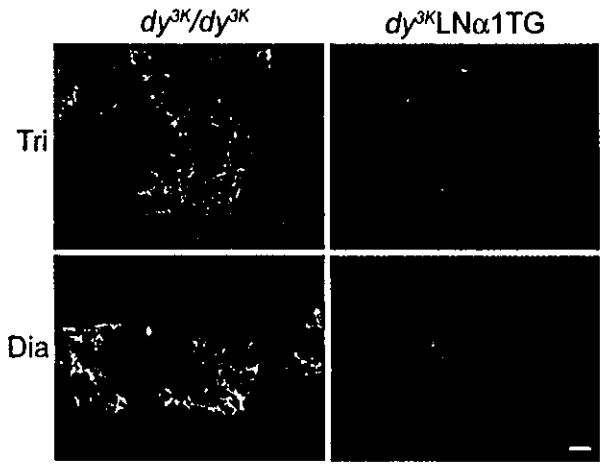

Figure 6. Immunostaining of tenascin-C. Cross-sections of triceps brachii (Tri) and diaphragm (Dia) from 4-month-old dy^{3K}LNα1TG mice and 3.5-week-old dy^{3K}/dy^{3K} mice were stained with antibodies against tenascin-C. Bar, 50 μm.

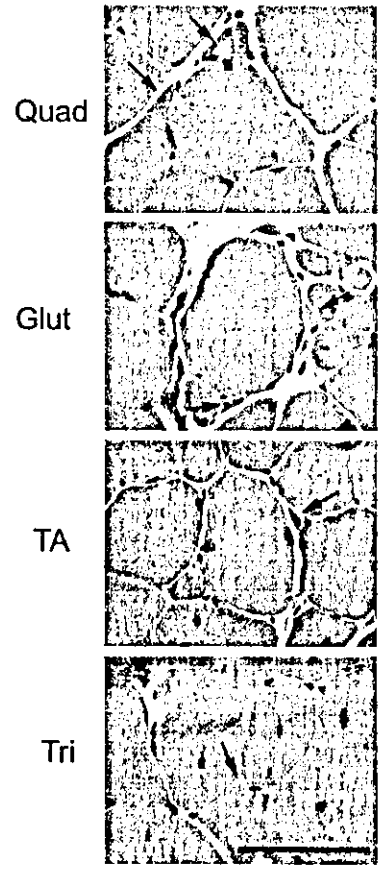

Figure 7. H&E staining of muscles from 4-month-old dy^{3K}LNα1TG mice reveals occasional neurogenic lesions. Cryosections of quadriceps femoris (Quad), gluteus maximus (Glut), tibialis anterior (TA) and triceps brachii (Tri) were stained with H&E. Arrows denote angular atrophic muscle fibers. Bar, 50 μm.

their hind legs to the trunk when lifted by the tail, an indication of a neurological problem. They also displayed hind leg paralysis, but to a varying degree (data not shown). In addition, we detected angular atrophic muscle fibers (indicating neurogenic lesions) in rescued muscles although they appeared rarely. As the LNα1 chain was not expressed in peripheral nerves of LNα1 chain transgenic mice, the nerve defect was not expected to be rescued. In this context, it is noteworthy that several attempts to express a LNα2 transgene in peripheral nerve have failed (9). Interestingly, loss of LNα2 chain in sciatic nerve of dy^{2J}/dy^{2J} mice was recently found to be accompanied by variable expression of LNα1 chain (47). Thus, it remains possible that overexpression of LNα1 chain can compensate for LNα2 chain deficiency also in peripheral nerves.

Apart for muscular dystrophy and peripheral neuropathy, LNα2 chain deficient mice also display central nervous system myelination defects, hearing loss and abnormal thymocyte and odontoblast development (13–15,48). It will now be interesting to investigate whether LNα1 chain can compensate for the absence of LNα2 chain in central nervous system, inner ear, thymus and tooth.

In conclusion, we have established that LNα1 chain significantly reduces muscular dystrophy in LNα2 chain deficient mice. Hence, our data suggest that LNα1 chain should be considered in the design of therapies to treat LNα2 chain deficient CMD. We also provide the first evidence that LNα chains functionally can compensate for each other *in vivo*.

MATERIALS AND METHODS

Transgenic construct

Full-length mouse LNα1 cDNA was generously provided by Dr P. Yurchenco (Robert Wood Johnson Medical School, Piscataway, NJ, USA) (49). *Eco*RI adaptors (Amersham-Pharmacia) were ligated to the ends of LNα1 chain cDNA, which was subsequently inserted to the *Eco*RI site of the expression vector pCAGGS containing a CMV enhancer and chicken β-actin promoter (generously provided by Dr J. Miyazaki, Osaka University Medical School, Osaka, Japan) (29). A 12 kb transgenic vector was released with *Sal*I and *Hind*III and used for one-cell embryo microinjection.

Production of LNα1 chain transgenic mice on wild-type background

Transgenic mice were generated by microinjections of transgene DNA into the pronucleus of fertilized single-cell CBAxC57BL/6 embryos (Karolinska Center of Transgene Technologies, Stockholm, Sweden). LNα1 transgenic mice were identified by Southern blot analysis using genomic DNA prepared from mouse tails and the probe indicated in Figure 1A. LNα1 positive founder transgenic mice were maintained in animal facilities according to animal care guidelines. The use of animals complied with national guidelines, and permission was given by the regional ethical board.

Production of transgenic mice on dy^{3K} background

Heterozygous LNα1 transgenic mice were bred to heterozygous dy^{3K}/+ mice (7), followed by sib breeding to generate mice heterozygous for the transgene and homozygous for dy^{3K}.

Genotyping

PCR on tail DNA was performed with LNα1 cDNA primer 5′-GGCATTGGGCGTGTCGAACAG-3′ and chicken β-actin primer 5′-GGTTCGGCTTCTGGCGTGTGA-3′, amplifying a 400 bp product for LNα1 chain positive transgenic mice. Dy^{3K} PCR was performed with primers 5′-CTTTCAGATT GCATTGCAAGC-3′ and 5′-CAATGCAGCTTTTTGATCTT AC-3′, which anneal to *Lama2* intron sequences flanking an exon (encoding a part of domain VI of LNα2 chain) that is disrupted by the insertion of a neo cassette in dy^{3K}/dy^{3K} mice (7). The PCR product is 1 kb for wild-type mice; 1 and 2.5 kb for heterozygous dy^{3K}/+ mice and 2.5 kb for homozygous dy^{3K}/dy^{3K} mice.

RT–PCR

Total RNA from skeletal muscle was isolated using TRIzol reagent (Invitrogen) according to manufacturer specifications. First strand cDNA synthesis from total RNA was performed using Superscript™ II RT (Invitrogen). PCR was perfomed using primers directed against LNα1 chain: 5′-ATATCACA CGCAATCGATGG-3′ and 5′-AGTAATAACGTCTTGTG-3′.

Exploratory locomotion

Exploratory locomotion was examined in an open field test. In each experiment a mouse was placed into a new cage and allowed to explore the cage for 5 min. The time that the mouse spent moving around was measured manually. For all experiments, each dy^{3K}LNα1TG animal ($n = 4$) was compared with a wild-type ($n = 4$) sibling of the same sex from the same litter.

Immunofluorescence

Tissues were immersed in Tissue Tek and frozen in liquid nitrogen. Cryosections (7 μm) were either stained with hemotoxylin and eosin (H&E) or analyzed by immunofluorescence. Primary antibodies were: anti-LNα1 chain mAb200 (50), anti tenascin-C MTn15 (50), anti-LNα2 chain 4H8-2 (Alexis Biochemicals), anti-LNα4 chain (generously provided by Dr R. Timpl), anti-LNα5 chain (generously provided by Dr R. Timpl), anti-LNβ2 chain (generously provided by Dr T. Sasaki) (51), anti-collagen type IV (Chemicon), anti-perlecan (generously provided by Dr R. Timpl), anti-α-dystroglycan IIH6C4 (Upstate Biotechnology). A rabbit polyclonal antibody was generated against the C-terminal 15 amino acids (KNMTPYRSPP-PYVPPC) of β-dystroglycan and affinity purified. For staining of NMJs, samples were simultaneously incubated with FITC-conjugated α-bungarotoxin (Molecular Probes). Images of sections analyzed by fluorescence microscopy (Zeiss Axioplan) were captured using an ORCA 1394 ER digital camera with Openlab 3 software. Images were prepared for publication using Adobe Photoshop software.

Transmission electron microscopy

Tibialis anterior muscles were fixed for 2 h with 2.5% glutaraldehyde, rinsed in Sörensen's phosphate buffer, post-fixed in 1% OsO_4 and then embedded in Epon. Ultra-thin sections were stained with uranyl acetate and lead citrate. Specimens were examined by transmission electron microscopy (Philips CM 10).

ACKNOWLEDGEMENTS

We thank P. Yurchenco, J. Miyazaki, T. Sasaki and the late R. Timpl for gifts of reagents and T. Hjalt and V. Allamand for critical reading of the manuscript. VR, Kungliga Fysiografiska Sällskapet, and Crafoord, Lars Hiertas Minne, Magnus Bergwall, and Åke Wibergs foundations funded this work.

REFERENCES

1. Colognato, H. and Yurchenco, P.D. (2000) Form and function: the laminin family of heterotrimers. *Dev. Dyn.*, **218**, 213–234.
2. Ekblom, P., Lonai, P. and Talts, J.F. (2003) Expression and biological role of laminin-1. *Matrix Biol.*, **22**, 35–47.
3. Gullberg, D., Tiger, C.F. and Velling, T. (1999) Laminins during muscle development and in muscular dystrophies. *Cell Mol. Life Sci.*, **56**, 442–460.
4. Helbling-Leclerc, A., Zhang, X., Topaloglu, H., Cruaud, C., Tesson, F., Weissenbach, J., Tome, F.M., Schwartz, K., Fardeau, M., Tryggvason, K. *et al.* (1995) Mutations in the laminin α2 chain gene (*LAMA2*) cause merosin-deficient congenital muscular dystrophy. *Nat. Genet.*, **11**, 216–218.
5. Allamand, V., Sunada, Y., Salih, M., Straub, V., Ozo, C., Al-Turaiki, M., Akbar, M., Kolo, T., Colognato, H., Zhang, X. *et al.* (1997) Mild congenital muscular dystrophy in two patients with an internally deleted laminin α2 chain. *Hum. Mol. Genet.*, **6**, 747–752.
6. Miyagoe-Suzuki, Y., Nakagawa, M. and Takeda, S. (2000) Merosin and congenital muscular dystrophy. *Microsc. Res. Tech.*, **48**, 181–191.
7. Miyagoe, Y., Hanaoka, K., Nonaka, I., Hayasaka, M., Nabeshima, Y., Arahata, K., Nabeshima, Y. and Takeda, S. (1997) Laminin α2 chain-null mutant mice by targeted disruption of the *Lama2* gene: a new model of merosin (laminin 2)-deficient congenital muscular dystrophy. *FEBS Lett.*, **415**, 33–39.
8. Kuang, W., Xu, H., Vachon, P.H., Liu, L., Loechel, F., Wewer, U. and Engvall, E. (1998) Merosin-deficient congenital muscular dystrophy. *J. Clin. Invest.*, **102**, 844–852.
9. Guo, L.T., Zhang, X.U., Kuang, W., Xu, H., Liu, L.A., Vilquin, J.-T., Miyagoe-Suzuki, Y., Takeda, S., Ruegg, M.A., Wewer, U. *et al.* (2003) Laminin α2 deficiency and muscular dystrophy: genotype–phenotype correlation in mutant mice. *Neuromuscul. Disord.*, **13**, 207–215.
10. Sunada, Y., Bernier, S.M., Kozak, C.A., Yamada, Y. and Campbell, K.P. (1994) Deficiency of merosin in dystrophic *dy* mice and genetic linkage of laminin M chain gene to *dy* locus. *J. Biol. Chem.*, **269**, 13729–13732.
11. Xu, H., Christmas, P., Wu, X.-R., Wewer, U.M. and Engvall, E. (1994) Defective muscle basement membrane and lack of M-laminin in the dystrophic *dy/dy* mouse. *Proc. Natl Acad. Sci. USA*, **91**, 5572–5576.
12. Besse, S., Allamand, V., Vilquin, J.-T., Zhenlin, L., Portier, C., Vignier, N., Hori, H., Guenet, J.-L. and Guicheney, P. (2003) Spontaneous muscular dystrophy caused by a retrotransposal insertion in the mouse laminin α2 chain gene. *Neuromuscul. Disord.*, **13**, 216–222.
13. Chun, S.J., Rasband, M.N., Sidman, R.L., Habib, A.A. and Vartanian, T. (2003) Integrin-linked kinase is required for laminin-2 induced

oligodendrocyte cell spreading and CNS myelination. *J. Cell Biol.*, **163**, 397–408.
14. Wagner, W.J., Chang, A.C., Owens, J., Hong, M.J., Brooks, A. and Coligan, J.E. (2000) Aberrant development of thymocytes in mice lacking laminin-2. *Dev. Immunol.*, **7**, 179–193.
15. Pillers, D.A., Kempton, J.B., Duncan, N.M., Pang, J., Dwinnel, S.J. and Trune, D.R. (2002) Hearing loss in the laminin-deficient dy mouse model of congenital muscular dystrophy. *Mol. Genet. Metab.*, **76**, 217–224.
16. Hartigan-O'Connor, D. and Chamberlain, J.S. (2000) Developments in gene therapy for muscular dystrophy. *Microsc. Res. Tech.*, **48**, 223–238.
17. Tinsley, J.M., Potter, A.C., Phelps, S.R., Fisher, R., Ticket, J.I. and Davies, K.E. (1996) Amelioration of the dystrophic phenotype of *mdx* mice using a truncated utrophin transgene. *Nature*, **384**, 349–353.
18. Patton, B., Miner, J.H., Chiu, A. and Sanes, J.R. (1997) Distribution and function of laminins in the neuromuscular system of developing, adult, and mutant mice. *J. Cell Biol.*, **15**, 1507–1521.
19. Noakes, P.G., Gautam, M., Mudd, J., Cunningham, J.M., Sanes, J.R. and Merlie, J.P. (1995) The renal glomerulus of mice lacking s-laminin/laminin β2 chain: nephrosis despite molecular compensation by laminin β1. *Nat. Genet.*, **10**, 400–406.
20. Miner, J.H., Cunningham, J. and Sanes, J.R. (1998) Roles for laminin in embryogenesis: exencephaly, syndactyly, and placentopathy in mice lacking the laminin α5 chain. *J. Cell Biol.*, **143**, 1713–1723.
21. Falk, M., Ferletta, M., Forsberg, E. and Ekblom, P. (1999) Restricted distribution of laminin α1 chain in normal adult mouse tissues. *Matrix Biol.*, **18**, 557–568.
22. Virtanen, I., Gullberg, D., Rissanen, J., Kivilaakso, E., Kiviluoto, T., Laitinen, L.A., Lehto, V.P. and Ekblom, P. (2000) Laminin α1-chain shows a restricted distribution in epithelial basement membranes of fetal and adult human tissues. *Exp. Cell Res.*, **257**, 298–309.
23. Miner, J.H., Lewis, R.M. and Sanes, J.R. (1995) Molecular cloning of a novel laminin chain, α5, and widespread expression in adult mouse tissues. *J. Biol. Chem.*, **270**, 28523–28526.
24. Kühl, U., Öcalan, M., Timpl, R. and von der Mark, K. (1986) Role of laminin and fibronectin in selecting myogenic versus fibrogenic cells from skeletal muscles *in vitro*. *Dev. Biol.*, **93**, 344–354.
25. Mayer, U. (2003) Integrins: redundant or important players in skeletal muscle? *J. Biol. Chem.*, **278**, 14587–14590.
26. Talts, J.F., Andac, Z., Gohring, W., Brancaccio, A. and Timpl, R. (1999) Binding of the G domains of laminin α1 and α2 chains and perlecan to heparin, sulfatides, α-dystroglycan and several extracellular matrix proteins. *EMBO J.*, **18**, 863–870.
27. Schuler, F. and Sorokin, L.M. (1995) Expression of laminin isoforms in mouse myogenic cells *in vitro* and *in vivo*. *J. Cell Sci.*, **108**, 3795–3805.
28. Vachon, P.H., Loechel, F., Xu, H., Wewer, U.M. and Engvall, E. (1996) Merosin and laminin in myogenesis: specific requirements for merosin in myotube stability and survival. *J. Cell Biol.*, **134**, 1483–1497.
29. Niwa, H., Yamamura, K. and Miyazaki, J. (1991) Efficient selection for high-expression transfectants with a novel eukaryotic vector. *Gene*, **108**, 193–200.
30. Tiger, C.F. and Gullberg, D. (1997) Absence of laminin α1 chain in the skeletal muscle of dystrophic *dy/dy* mice. *Muscle Nerve*, **20**, 1515–1524.
31. Moll, J., Barzaghi, P., Lin, S., Bezakova, G., Lochmuller, H., Engvall, E., Muller, U. and Ruegg, M.A. (2001) An agrin minigene rescues dystrophic symptoms in a mouse model for congenital muscular dystrophy. *Nature*, **413**, 302–307.
32. Michelson, A.M., Russel, E. and Harman, P.J. (1955) Dystrophia muscularis: a hereditary primary myopathy in the house mouse. *Proc. Natl Acad. Sci. USA*, **41**, 1079–1084.
33. Cohn, R.D., Herrmann, R, Wewer, U.M. and Voit, T. (1997) Changes of laminin β2 chain expression in congenital muscular dystrophy. *Neuromuscul. Disord.*, **7**, 373–378.
34. Ferletta, M., Kikkawa, Y., Yu, H., Talts, J.F., Durbeej, M., Sonnenberg, A., Timpl, R., Campbell, K.P., Ekblom, P. and Genersch, E. (2003) Opposing roles of integrin α6Aβ1 and dystroglycan in laminin-mediated extracellular signal-regulated kinase activation. *Mol. Biol. Cell*, **14**, 2088–2103.
35. Connolly, A.M., Keeling, R.M., Mehta, S., Pestronk, A. and Sanes, J.R. (2001) Three mouse models of muscular dystrophy: the natural history of strength and fatigue in dystrophin-, dystrophin/utrophin-, and laminin α2 deficient mice. *Neuromuscul. Disord.*, **11**, 703–712.
36. Cossu, G. and Mavilio, F. (2000) Myogenic stem cells for the therapy of primary myopathies: wishful thinking or therapeutic perspective? *J. Clin. Invest.*, **105**, 1669–1674.
37. Ringelman, B., Röder, C., Hallmann, R., Maley, M., Davies, M., Grounds, M. and Sorokin, L.M. (1999) Expression of laminin α1, α2, α4, and α5 chains, fibronectin, and tenascin-C in skeletal muscle of dystrophic 129ReJ *dy/dy* mice. *Exp. Cell Res.*, **246**, 165–182.
38. Nakagawa, M., Miyagoe-Suzuki, Y., Ikezoe, K., Miyata, Y., Nonaka, I., Harii, K. and Takeda, S. (2001) Schwann cell myelination occurred without basal lamina formation in laminin α2 chain-null mutant (*dy3K/dy3K*) mice. *Glia*, **35**, 101–110.
39. Bradley, W.G. and Jenkinson, M. (1975) Abnormalities of peripheral nerves in murine muscular dystrophy. *J. Neurol. Sci.*, **18**, 227–247.
40. Shorer, Z., Philpot, J., Muntoni, F., Sewry, C. and Dubowitz, V. (1995) Demyelinating peripheral neuropathy in merosin-deficient congenital muscular dystrophy. *J. Child Neurol.*, **10**, 472–475.
41. Öcalan, M., Goodman, S.L., Kühl, U., Hauschka, S.D. and von der Mark, K. (1988) Laminin alters cell shape and stimulates motility and proliferation of murine skeletal myoblasts. *Dev. Biol.*, **125**, 58–67.
42. Durbeej, M. and Campbell, K.P. (2002) Muscular dystrophies involving the dystrophin–glycoprotein complex: an overview of current mouse models. *Curr. Opin. Genet. Dev.*, **12**, 349–361.
43. DelloRusso, C., Scott, J.M., Hartigan-O'Connor, D., Salvatori, G., Barjot, C., Robinson, A.S., Crawford, R.W., Brooks, S.V. and Chamberlain, J.S. (2002) Functional correction of adult *mdx* mouse muscle using gutted adenoviral vectors expressing full-length dystrophin. *Proc. Natl Acad. Sci. USA*, **99**, 12979–12984.
44. Li, X., Talts, U., Talts, J.F., Arman, E., Ekblom, P. and Lonai, P. (2001) Akt/PKB regulates laminin and collagen IV isotypes of the basement membrane. *Proc. Natl Acad. Sci. USA*, **98**, 14416–14421.
45. Lawlor, M.A. and Alessi, D.R. (2001) PKB/Akt: a key mediator of cell proliferation, survival and insulin responses? *J. Cell Sci.*, **114**, 2903–2910.
46. Niimi, T., Hayashi, Y. and Sekiguchi, K. (2003) Identification of an upstream enhancer in the mouse laminin α1 gene defining its high level of expression in parietal endoderm cells. *J. Biol. Chem.*, **278**, 9332–9338.
47. Previtali, S.C., Nodari, A., Taveggia, C., Pardini, C., Dina, G., Villa, A., Wrabetz, L., Quattrini, A. and Feltri, M.L. (2003) Expression of laminin receptors in schwann cell differentiation: evidence for distinct roles. *J. Neurosci.*, **23**, 5520–5530.
48. Yuasa, K., Fukumoto, S., Kamasaki, Y., Yamada, A., Fukumoto, E., Kanaoka, K., Saito, K., Harada, H., Arikawa-Hirasawa, E., Miyagoe-Suzuki, Y. *et al.* (2004) Laminin α2 is essential for odontoblast differentiation regulating dentin sialoprotein expression. *J. Biol. Chem.*, **279**, 10286–10292.
49. Yurchenco, P.D., Quan, Y., Colognato, H., Mathus, T., Harrison, D., Yamada, Y. and O'Rear, J.J. (1997) The α chain of laminin-1 is independently secreted and drives secretion of its β- and γ-chain partners. *Proc. Natl Acad. Sci. USA*, **16**, 10189–10194.
50. Kadoya, Y., Kadoya, K., Durbeej, M., Holmvall, K., Sorokin, L. and Ekblom, P. (1995) Antibodies against domain E3 of laminin-1 and integrin α6 subunit perturb branching epithelial morphogenesis of submandibular glands but by different modes. *J. Cell Biol.*, **129**, 521–534.
51. Sasaki, T., Mann, K., Miner, J.H., Miosge, N. and Timpl, R. (2002) Domain IV of mouse laminin β1 and β2 chains. *Eur. J. Biochem.*, **269**, 431–442.

Available online at www.sciencedirect.com
SCIENCE DIRECT
Experimental Cell Research 296 (2004) 245–255
Experimental Cell Research
www.elsevier.com/locate/yexcr

Purification and cell-surface marker characterization of quiescent satellite cells from murine skeletal muscle by a novel monoclonal antibody

So-ichiro Fukada,[a] Saito Higuchi,[a] Masashi Segawa,[a] Ken-ichi Koda,[a] Yukiko Yamamoto,[a] Kazutake Tsujikawa,[a] Yasuhiro Kohama,[a] Akiyoshi Uezumi,[b] Michihiro Imamura,[b] Yuko Miyagoe-Suzuki,[b] Shin'ichi Takeda,[b] and Hiroshi Yamamoto[a,*]

[a] *Department of Immunology, Graduate School of Pharmaceutical Sciences, Osaka University, Suita, Osaka 565-0871, Japan*
[b] *Department of Molecular Therapy, National Institute of Neuroscience, National Center of Neurology and Psychiatry, Kodaira, Tokyo 187-8502, Japan*

Received 10 November 2003; received in revised form 16 February 2004

Available online 25 March 2004

Abstract

A novel monoclonal antibody, SM/C-2.6, specific for mouse muscle satellite cells was established. SM/C-2.6 detects mononucleated cells beneath the basal lamina of skeletal muscle, and the cells co-express M-cadherin. Single fiber analyses revealed that M-cadherin$^+$ mononucleated cells attaching to muscle fibers are stained with SM/C-2.6. SM/C-2.6$^+$ cells, which were freshly purified by FACS from mouse skeletal muscle, became MyoD$^+$ in vitro in proliferating medium, and the cells differentiated into desmin$^+$ and nuclear-MyoD$^+$ myofibers in vitro when placed under differentiation conditions. When the sorted cells were injected into *mdx* mouse muscles, donor cells differentiated into muscle fibers. Flow cytometric analyses of SM/C-2.6$^+$ cells showed that the quiescent satellite cells were c-kit$^-$, Sca-1$^-$, CD34$^+$, and CD45$^-$. More, SM/C-2.6$^+$ cells were barely included in the side population but in the main population of cells in Hoechst dye efflux assay. These results suggest that SM/C-2.6 identifies and enriches quiescent satellite cells from adult mouse muscle, and that the antibody will be useful as a powerful tool for the characterization of cellular and molecular mechanisms of satellite cell activation and proliferation.

Keywords: Cell surface marker; Satellite cell; Skeletal muscle; Stem cell

Introduction

During the last decade, many reports have described the existence of tissue-specific stem cells that are able to self-renew and generate committed progenitors. Hematopoietic stem cells in bone marrow are well-characterized and defined as c-kit$^+$, Sca-1$^+$, and Lin$^-$ [1,2], and bone marrow transplantation is now clinically applied to various immunological and hematological disorders. In addition to hematopoietic stem cells, bone marrow contains mesenchymal stem cells that have been characterized by their ability to differentiate into various types of tissue-specific cells in both in vitro and in vivo experiments. Mesenchymal stem cells can generate bone, cartilage, connective tissue [3–7], and cardiomyocytes [8]. Cord blood also contains mesenchymal stem cells [9–11] and this also forms various mesenchymal tissue cells in vitro.

It is widely accepted that the postnatal growth and repair of skeletal muscle is normally mediated by satellite cells that locate between the basal lamina and sarcolemma of myofibers [12–14]. Thus, satellite cells have been considered to be the only myogenic source for the maintenance of skeletal muscle [15,16]. Satellite cells can be enriched by culturing cells from enzymatically digested muscles [17–21]. When muscle regeneration starts, the state of the satellite cells changes from resting or quiescent to activated and proliferative. However, the conditions under which the activation and the proliferation of satellite cells are initiated have not yet been well characterized.

The myogenic potential of mesenchymal stem cells from rat bone marrow in both in vivo [22] and in vitro experiments [23] has been described. These results prompted speculation

Abbreviations: GFP-Tg, Green fluorescent protein gene transgenic; MAb, Monoclonal antibody; MP, Main population; SP, Side population; TA, Tibialis anterior.

* Corresponding author. Department of Immunology, Graduate School of Pharmaceutical Sciences, Osaka University, 1-6 Yamada-oka, Suita, Osaka 565-0871, Japan. Fax: +81-6-6879-8194.
E-mail address: hiroshiy@phs.osaka-u.ac.jp (H. Yamamoto).

0014-4827/$ - see front matter © 2004 Elsevier Inc. All rights reserved.
doi:10.1016/j.yexcr.2004.02.018

that the transplanted bone marrow cells can move to damaged muscle and grow into new muscle fibers in mice [24]. Recently, several investigators have reported that transplanted bone marrow cells participate in the muscle regeneration process in irradiated or neonatal recipient mice [25–28]. These procedures opened new pathways for tissue reconstitution therapy via cell transplantation, however, muscle fibers containing donor cell-derived markers were still too low to treat patients with primary myopathies. Very recently, Asakura et al. and others reported the possibility that other muscle stem cells, so-called side population (SP) cells, might exhibit the potential to give rise to myocytes and satellite cells in transplanted muscle [26,29,30]. Thus, the possible interchange among bone marrow cells, muscle SP cells, and satellite cells has received increasing attention from the viewpoint of understanding muscle-specific stem cell biology.

To investigate the molecular events involved in the stimulation and differentiation of satellite cells, it is important to isolate satellite cells from fresh muscles. In this report, we describe the novel monoclonal antibody, SM/C-2.6, that specifically detects satellite cells. SM/C-2.6-positive cells sorted from fresh muscle generated muscle fibers both in vitro and in vivo, and the surface phenotypes of satellite cells were defined.

Materials and methods

Animals and cells

Specific pathogen-free C3H/HeN and C57BL/6 mice aged 6 to 8 weeks were purchased from Charles River Japan (Yokohama, Japan). Specific pathogen-free *mdx* mice (of C57BL/10 background) were provided by Central Laboratories for Experimental Animals (Kanagawa, Japan). C3H/HeN newborn mice were prepared in our animal facility by brother–sister mating. Heterozygous EGFP transgenic (GFP-Tg) mice with a C57BL/6 background [31] were maintained in our animal facility by mating with normal C57BL/6 mice. Sprague–Dawley rats were purchased from CLEA Japan (Tokyo, Japan).

The mouse myogenic cell line C2/4, a subline of C2C12, was a gift from Dr. S. Yoshida (Kyoto University, Kyoto, Japan) and was maintained in culture in 10% FCS containing DMEM medium. A mouse hepatocyte cell line, NCTC1469 [32], was obtained from the Japanese Collection of Research Bioresources, National Institute of Health Sciences, Tokyo, Japan.

Freshly isolated muscle-derived cells from neonatal and adult mice were prepared according to the methods of Rando and Blau [33]. Muscles from neonatal and adult mice were isolated and digested with collagenase type II (Worthington Biochemical Corp., Lakewood, NJ) for 90 min at 37°C. We triturated muscle tissues every 15 min during 90 min incubation and passed through a 37-μm nylon mesh. Single cell suspensions were washed and stained with various mAbs. We usually obtained approximately 5×10^6 cells from 1 g of muscle of 8-week-old female C57BL/6 mice. Sorted cells were obtained from GFP-Tg mice and injected into the tibialis anterior (TA) muscles of *mdx* mice. Two weeks later, the muscles were isolated, frozen in liquid nitrogen-cooled isopentane, and cryosections were examined histologically. Cryosections were examined for GFP^+ muscle fibers under a confocal laser-scanning microscope (model MRC1024ES, Bio-Rad Laboratories, Hercules, CA).

Antibodies

A rat mAb to mouse c-kit (ACK2) [34] was a gift from Dr. S-I. Nishikawa (Kyoto University); it was labeled with FITC in our laboratory. Anti-Sca-1-PE (E13-161.7), anti-CD34-FITC (RAM34), anti-CD45-PE (30-F11), and anti-MyoD (MoAb 5.8A) were purchased from Pharmingen (San Diego, CA). A rabbit anti-mouse M-cadherin polyclonal antibody was prepared in our laboratory. A rabbit anti-mouse laminin polyclonal antibody and TRITC-conjugated goat anti-mouse immunoglobulin were purchased from LSL Co., Ltd. (Tokyo, Japan) and Chemicon International, Inc. (Temecula, CA), respectively. Rhodamine-Red TM-X conjugated goat anti-rabbit IgG and Alexa488-conjugated goat anti-rabbit IgG were purchased from Molecular Probes Inc. (Eugene, OR). A rabbit anti-desmin polyclonal antibody and FITC-conjugated goat anti-rat IgG were purchased from ICN Pharmaceuticals, Inc.-Cappel Products (Aurora, OH). Monoclonal anti-dystrophin (MANDRA-1, Sigma) was labeled with a fluorochrome Alexa 568 in our laboratory. R-PE-streptavidin (Molecular Probes) or FITC-streptavidin (Pharmingen) was used to detect biotinylated antibodies. Anti-human c-met mAb (DO-24) reactive to mouse c-met [35] was purchased from Upstate (Lake Placid, NY), and it was used with Alexa488-conjugated goat anti-mouse IgG (H+L) (Molecular Probes).

Establishment of monoclonal antibodies

MAbs were established according to a standard procedure. Briefly, $1–2 \times 10^6$ C2/4 cells were injected intraperitoneally into Sprague–Dawley rats seven times at weekly intervals. Three days after the last injection, the rats were sacrificed under ether anesthesia and splenocytes were fused with partner cells, P3X63Ag8U.1 (P3U1). Strategies for mAb selection are described in Results. Finally, a mAb clone, SM/C-2.6, was established.

Flow cytometry and cell sorting

Regular flow cytometric profiles were analyzed with a FACSCalibur analyzer and CELLQuest software (Becton Dickinson Immunocytometry Systems, Mountain View, CA). SM/C2.6-reactive mononuclear cells were fractionated on a fluorescent-activated cell sorter (EPICS Elite, Coulter Electronics, Hialeah, FL). Dead cells were excluded from

the plots based on propidium iodide staining (Sigma Co., St. Louis, MO).

Hoechst staining was performed as described by Goodell et al. (http://www.bcm.tmc.edu/genetherapy/goodell/newsite/protocols.html). In brief, hindlimb muscles of 8 week-old C57BL/6 mice were digested with collagenase type II (Worthington Biochemical), suspended at 10^6 cells per ml in Dulbecco's modified Eagle's medium (DME) (Gibco BRL, Grand Island, NY) containing 2% fetal calf serum (FCS, Boehringer-Mannheim GmbH, Mannheim, Germany), 10 mM Hepes, and 5 μg/ml Hoechst 33342 (Sigma), and incubated at 37°C for 90 min in the presence or absence of 50 μM verapamil (Sigma). After Hoechst staining, the cells were washed and stained with biotinylated-SM/C-2.6 and FITC-streptavidin (Pharmingen). Flow cytometric analyses were performed on FACSVantageSE (Becton Dickinson). Hoechst 33342 was excited with a multi-line UV laser (351.1–363.8 nm) and its fluorescence was measured with a 424/44 BP filter and 675/20 BP filter. FITC and PI were excited at 488 nm by an Ar laser, and measured with 530/30 BP and 630/22 BP filters, respectively.

Immunohistochemistry

For immunohistochemical examinations of muscles, cryosections (6 μm) were fixed in acetone for 10 min and incubated in 5% skim milk for 10 min to block nonspecific antibody binding. SM/C-2.6, anti-laminin, anti-M-cadherin, and anti-dystrophin antibodies were applied to the sections for 60 min at 37°C. SM/C-2.6 mAb was detected by FITC-conjugated goat anti-rat IgG as a second antibody. Anti-laminin and anti-M-cadherin antibodies were detected by Rhodamine Red TM-X conjugated goat anti-rabbit IgG. The signals were recorded photographically using an Axiophot microscope (Carl Zeiss, Oberkochen, Germany).

Isolation and immunostaining of single fibers

To detect muscle satellite cells attaching single fibers with SM/C-2.6 and M-cadherin, muscle fibers from extensor digitorium longus (EDL) muscles of C3H/HeN mice were prepared essentially according to the methods of Bischoff [17] and Rosenblatt et al. [18]. Briefly, dissected muscle was incubated with 0.5% type I collagenase (Worthington) in DME at 37°C for 90 min. The muscle mass was transferred to fresh growth medium, high-glucose DME containing 10% FCS and penicillin (200 U/ml)–streptomycin (200 μg/ml) (Gibco BRL). The muscle mass was then triturated with a fire-polished wide-mouth Pasteur pipette. Fibers were transferred to a Matrigel (Collaborative Biomedical, Bedford, MA)-coated Lab-Tek chamber (Nalge Nunc International, Naperville, IL) and fixed in 4% paraformaldehyde in PBS for 5 min at room temperature. Fibers were permeabilized with 0.5% Triton X-100 (Nacalai Tesque, Kyoto, Japan) in PBS at room temperature for 20 min, then the nonspecific binding was blocked by incubation with 5% skim milk (in PBS) for 10 min. SM/C-2.6 and anti-M-cadherin antibodies were applied for 60 min at 37°C. Antibodies were detected using the second antibodies described in the earlier section.

Immunostaining of cultured cells

SM/C-2.6-reactive cells were fractionated on a cell sorter (EPICS Elite, Coulter Electronics), cultured, and then fixed with 2% PFA in PBS at room temperature for 10 min. Cells were permeabilized with 0.25% Triton X-100 in PBS at room temperature and then incubated in 5% skim milk for 10 min. Anti-MyoD and anti-desmin antibodies were added for 60 min at 37°C. Anti-MyoD mAb was detected using TRITC-conjugated goat anti-mouse IgG, and anti-desmin antibody was detected by Alexa 488-conjugated goat anti-rabbit IgG.

Results

Novel monoclonal antibody SM/C-2.6 detects skeletal muscle satellite cells

Satellite cell-specific mAbs were screened in three successive steps. First, mAbs that reacted to C2/4 (C2C12) immunogen were selected by flow cytometry. Second, mAbs that stained mouse thymocytes were discarded to exclude clones reactive to common mouse antigens. At this step, clones reactive to most mouse bone marrow cells were also discarded. Last, the clones reactive to mononuclear cells beneath the basal lamina of mouse skeletal muscles were selected immunohistochemically, and finally, we established the mAb SM/C-2.6. Flow cytometric data show that SM/C-2.6 stains C2/4 (Fig. 1Aa) and a fraction of bone marrow cells (approximately 10%) (Fig. 1Ac), but not thymocytes (Fig. 1Ab). SM/C-2.6 detects mononuclear cells residing beneath the laminin-positive basal lamina of muscle (Figs. 1Ba–c). This is the typical position at which muscle satellite cells reside. SM/C-2.6-positive cells (Fig. 1Bd) were also stained by M-cadherin (Fig. 1Be), which is a typical marker molecule for satellite cells. To confirm that the cells were satellite cells, we isolated living single fibers and stained them with SM/C-2.6. SM/C-2.6-stained mononuclear cells on freshly isolated single fibers. The SM/C-2.6-positive cells attached to a single fiber (Fig. 1Bg) were also stained by M-cadherin (Fig. 1Bh). The myonuclei visualized by counterstaining with DAPI expressed neither SM/C-2.6 nor M-cadherin (Fig. 1Bi).

SM/C-2.6-positive cells differentiate to myoblasts and myotubes in vitro

To determine whether SM/C-2.6-positive cells express other muscle-related molecules, we next fractionated the

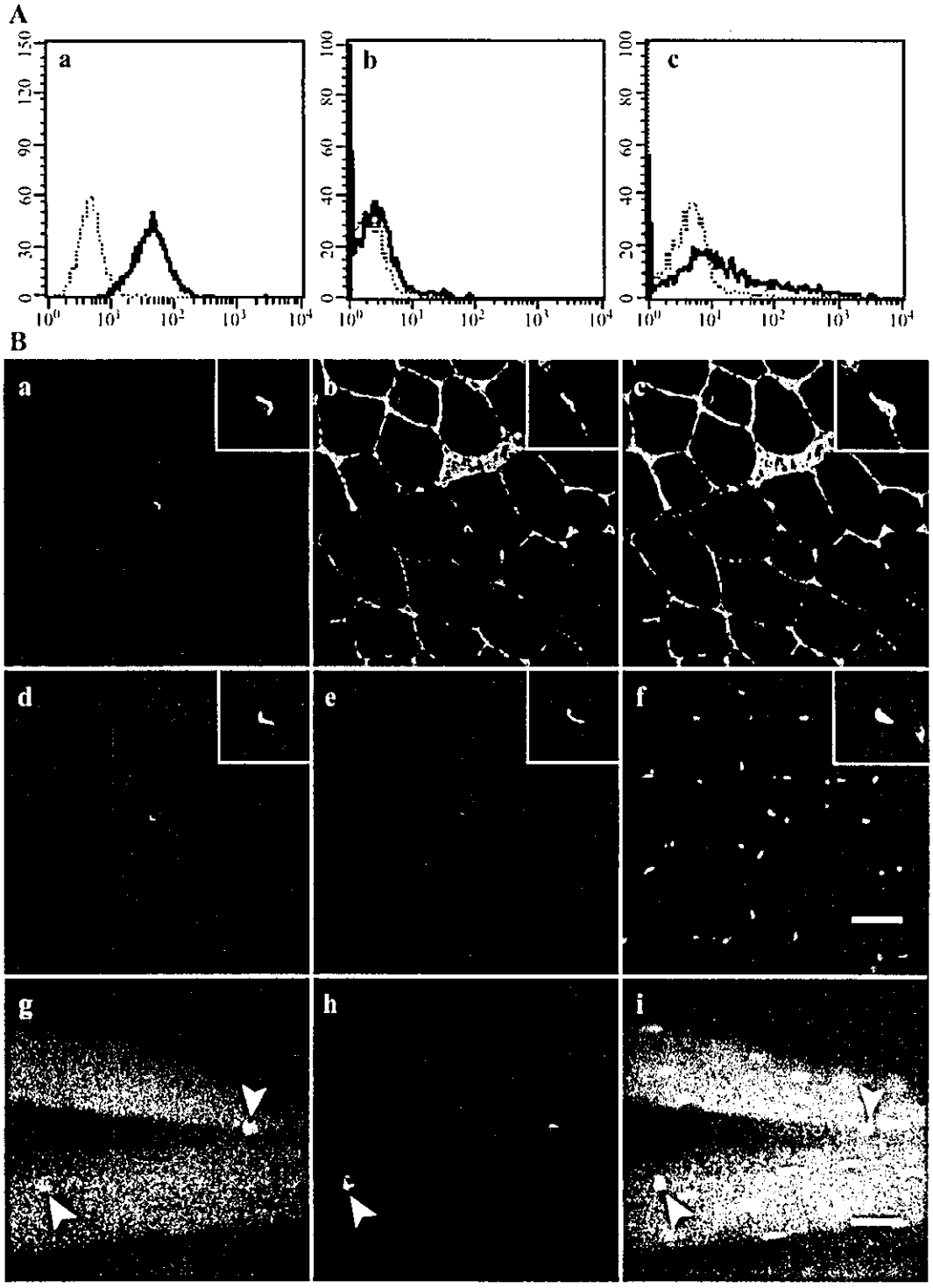

Fig. 1. Establishment of a novel monoclonal antibody, SM/C-2.6. A: SM/C-2.6 reacts with C2/4 cells (a) and a population of bone marrow cells (c), but not with thymocytes (b). Thin lines; control, thick lines; SM/C-2.6. B: Muscle satellite cells were stained with SM/C-2.6. Adult mouse muscle was stained with SM/C-2.6 (a, d), laminin (b), DAPI (c) (merged with a and b), M-cadherin (e), and DAPI (f) (merged with d and e). SM/C-2.6-reactive cells reside beneath the laminin layer and co-stained with anti-M-cadherin antibody. Single fibers from adult EDL muscle were stained with SM/C-2.6 (g), M-cadherin (h), and DAPI (merged with g and h) (i). SM/C-2.6-positive single cells attached to fibers were also stained with M-cadherin. SM/C-2.6 and M-cadherin-positive nuclei are distinguishable from myonuclei (i). Scale bars: 50 μm (a–i).

neonatal mouse muscle-derived mononuclear cells into SM/C-2.6-positive and -negative populations by using FACS sorting and cultured them in vitro. Neonatal muscle contains approximately 25% SM/C-2.6-positive cells (shown later, Fig. 4a). The positively and negatively sorted fractions contain more than 90% and less than 1% SM/C-2.6-positive